

**Sequential C–H and C–Ru Bond Formation and  
Cleavage during the Thermally Induced Rearrangement  
of Aryl Ruthenium(II) Complexes with  
[C<sub>6</sub>H<sub>3</sub>(CH<sub>2</sub>NMe<sub>2</sub>)<sub>2-2,6</sub>]<sup>−</sup> as a Bidentate  $\eta^2$ -C,N Coordinated  
Ligand. The Crystal Structures of the Isomeric Pairs  
[RuCl{ $\eta^6$ -C<sub>10</sub>H<sub>14</sub>}{ $\eta^2$ -C,N-C<sub>6</sub>H<sub>3</sub>(CH<sub>2</sub>NMe<sub>2</sub>)<sub>2-2,n</sub>}] (*n* = 4 or 6)  
and [Ru( $\eta^5$ -C<sub>5</sub>H<sub>5</sub>){ $\eta^2$ -C,N-C<sub>6</sub>H<sub>3</sub>(CH<sub>2</sub>NMe<sub>2</sub>)<sub>2-2,n</sub>}(PPh<sub>3</sub>)] (*n* =  
4 or 6)**

Pablo Steenwinkel,<sup>†</sup> Stuart L. James,<sup>†</sup> Robert A. Gossage,<sup>†</sup> David M. Grove,<sup>†</sup>  
Huub Kooijman,<sup>‡</sup> Wilberth J. J. Smeets,<sup>‡</sup> Anthony L. Spek,<sup>1,‡</sup> and  
Gerard van Koten<sup>\*,†</sup>

*Debye Institute, Department of Metal-Mediated Synthesis, and Bijvoet Institute for  
Biomolecular Research, Department of Crystal and Structural Chemistry, Utrecht University,  
Padualaan 8, 3584 CH, Utrecht, The Netherlands*

Received May 4, 1998

New air-stable ruthenium(II) complexes that contain the arylidiamine ligand [C<sub>6</sub>H<sub>3</sub>(CH<sub>2</sub>NMe<sub>2</sub>)<sub>2-2,6</sub>]<sup>−</sup> (NCN) are described. These complexes are [RuCl{ $\eta^2$ -C,N-C<sub>6</sub>H<sub>3</sub>(CH<sub>2</sub>NMe<sub>2</sub>)<sub>2-2,6</sub>}( $\eta^6$ -C<sub>10</sub>H<sub>14</sub>)] (**2**; C<sub>10</sub>H<sub>14</sub> = *p*-cymene = C<sub>6</sub>H<sub>4</sub>Me-*Pr*-4), [Ru{ $\eta^2$ -C,N-C<sub>6</sub>H<sub>3</sub>(CH<sub>2</sub>NMe<sub>2</sub>)<sub>2-2,6</sub>}( $\eta^5$ -C<sub>5</sub>H<sub>5</sub>)(PPh<sub>3</sub>)] (**5**), and their isomeric forms [RuCl{ $\eta^2$ -C,N-C<sub>6</sub>H<sub>3</sub>(CH<sub>2</sub>NMe<sub>2</sub>)<sub>2-2,4</sub>}( $\eta^6$ -C<sub>10</sub>H<sub>14</sub>)] (**3**) and [Ru{ $\eta^2$ -C,N-C<sub>6</sub>H<sub>3</sub>(CH<sub>2</sub>NMe<sub>2</sub>)<sub>2-2,4</sub>}( $\eta^5$ -C<sub>5</sub>H<sub>5</sub>)(PPh<sub>3</sub>)] (**6**), respectively. Complex **2** has been prepared from the reaction of [Li(NCN)]<sub>2</sub> with [RuCl<sub>2</sub>( $\eta^6$ -C<sub>10</sub>H<sub>14</sub>)]<sub>2</sub>, whereas complex **5** has been prepared by the treatment of [RuCl{ $\eta^3$ -N,C,N-C<sub>6</sub>H<sub>3</sub>(CH<sub>2</sub>NMe<sub>2</sub>)<sub>2-2,6</sub>}(PPh<sub>3</sub>)] (**4**) with [Na(C<sub>5</sub>H<sub>5</sub>)]<sub>*n*</sub>. Both **2** and **5** are formally 18-electron ruthenium(II) complexes in which the monoanionic potentially tridentate coordinating ligand NCN is  $\eta^2$ -C,N-bonded. In solution (halocarbon solvent at room temperature or in aromatic solvents at elevated temperature), the intramolecular rearrangements of **2** and **5** afford complexes **3** and **6**, respectively. This is a result of a shift of the metal–C<sub>aryl</sub> bond from position-1 to position-3 on the aromatic ring of the NCN ligand. The mechanism of the isomerization is proposed to involve a sequence of intramolecular oxidative addition and reductive elimination reactions of both aromatic and aliphatic C–H bonds. This is based on results from deuterium labeling, spectroscopic studies, and some kinetic experiments. The mechanism is proposed to contain fully reversible steps in the case of **5**, but a nonreversible step involving oxidative addition of a methyl NCH<sub>2</sub>–H bond in the case of **2**. The solid-state structures of complexes **2**, **3**, **5**, and **6** have been determined by single-crystal X-ray diffraction. A new dinuclear 1,4-phenylene-bridged bisruthenium(II) complex, [1,4-{RuCl( $\eta^6$ -C<sub>10</sub>H<sub>14</sub>)}<sub>2</sub>{C<sub>6</sub>(CH<sub>2</sub>NMe<sub>2</sub>)<sub>4-2,3,5,6</sub>-C,N,C',N'}] (**9**) has also been prepared from the dianionic ligand [C<sub>6</sub>(CH<sub>2</sub>NMe<sub>2</sub>)<sub>4-2,3,5,6</sub>]<sup>2−</sup> (C<sub>2</sub>N<sub>4</sub>). The C<sub>2</sub>N<sub>4</sub> ligand is in an  $\eta^2$ -C,N- $\eta^2$ -C',N'-bis(bidentate) bonding mode. Compound **9** does not isomerize in solution (halocarbon solvent), presumably because of the absence of an accessible C<sub>aryl</sub>–H bond. Complex **9** could not be isolated in an analytically pure form, probably because of its high sensitivity to air and very low solubility, which precludes recrystallization.

### Introduction

Recently, we have been focusing on the development of homogeneous catalysts and energy-transfer systems incorporating anionic multidentate aryl ligand

systems.<sup>1–4</sup> These ligand fragments include [4,4'-{C<sub>6</sub>H<sub>2</sub>(CH<sub>2</sub>NMe<sub>2</sub>)<sub>2-2,6</sub>]<sub>2</sub>]<sup>2−</sup> (**A**), [C<sub>6</sub>(CH<sub>2</sub>NMe<sub>2</sub>)<sub>4-2,3,5,6</sub>]<sup>2−</sup>

\* To whom correspondence should be addressed. E-mail: g.vankoten@chem.uu.nl. Fax: +31-30-2523615. Phone: + 31-30-2533120.

<sup>†</sup> To whom correspondence pertaining to crystallographic studies should be addressed. E-mail: spea@xray.chem.uu.nl.

<sup>‡</sup> Debye Institute.

<sup>§</sup> Bijvoet Institute for Biomolecular Research.

(1) (a) van Koten, G. *Pure Appl. Chem.* **1989**, *61*, 1681. (b) Rietveld, M. H. P.; Grove, D. M.; van Koten, G. *New J. Chem.* **1997**, *21*, 751. (c) Steenwinkel, P.; Gossage, R. A.; van Koten, G. *Chem. Eur. J.* **1998**, *4*, 759.

(2) (a) Steenwinkel, P.; James, S. L.; Veldman, N.; Kooijman, H.; Spek, A. L.; Grove, D. M.; van Koten, G. *Organometallics* **1997**, *16*, 513. (b) Steenwinkel, P.; Jastrzebski, J. T. B. H.; Deelman, B.-J.; Grove, D. M.; Kooijman, H.; Veldman, N.; Smeets, W. J. J.; Spek, A. L.; van Koten, G. *Ibid.* **1997**, *16*, 5486. (c) Lagunas, M.-C.; Gossage, R. A.; Spek, A. L.; van Koten, G. *Ibid.* **1998**, *17*, 731.

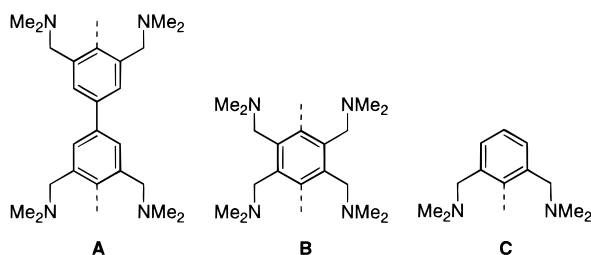
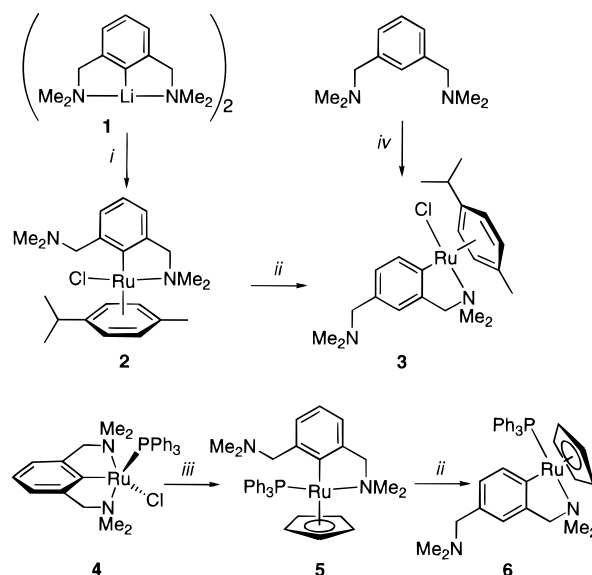


**Figure 1.** Schematic representation of the dianionic potentially bis-tridentate coordinating ligands bis-NCN (**A**) and  $C_2N_4$  (**B**) and the monoanionic potentially tridentate coordinating NCN ligand (**C**).

(**B**:  $C_2N_4$ ), and  $[C_6H_3(CH_2NMe_2)_{2-2,6}]^-$  (**C**: NCN), which are depicted in Figure 1. All of these species are representatives of a general class of organic fragments that are commonly referred to as the “pincer” ligands.<sup>1c</sup>

These investigations have led to the development of several general routes for the introduction of metal centers into these frameworks.<sup>1–3</sup> Specifically, this work has included the preparation and characterization of a number of novel aryl ruthenium(II) complexes,<sup>3,4</sup> some of which have interesting catalytic activity.<sup>5</sup> Herein, two new organoruthenium(II) complexes of NCN and one of  $C_2N_4$  are reported. In both cases, the coordination of these ligands involves  $\eta^2$ -C,N bonding to the metal center(s). Unexpectedly, the mononuclear complexes of NCN undergo selective thermal rearrangement (i.e., isomerization) chemistry involving the metallated aryl ligand, the course of which depends on other auxiliary ligands. Since our goals include the synthesis of novel complexes for applications in catalysis,<sup>5</sup> there is concern about the formation of isomers and/or other compounds during reactivity. If the rearrangement of a substrate, product, or catalysts is a competing process during catalysis, then this isomerization may have a profound impact on the resulting product distribution.<sup>6,7</sup> The formation of inactive or insoluble isomers can also

**Scheme 1.** Synthesis and Thermal Rearrangement of Ruthenium(II) Complexes **2** and **5** to the Isomeric Complexes **3** and **6**, and an Alternative Preparation of Complex **3**<sup>a</sup>



<sup>a</sup> Conditions: (i)  $[RuCl_2(\eta^6-C_{10}H_{14})]_2$ , Et<sub>2</sub>O, RT; (ii) C<sub>6</sub>H<sub>6</sub>, reflux; (iii)  $[Na(C_5H_5)]_n$ , THF, RT; (iv)  $[RuCl_2(\eta^6-C_{10}H_{14})]_2$ , NaPF<sub>6</sub>, CH<sub>2</sub>Cl<sub>2</sub>, RT.

lead to catalyst deactivation and/or to drastic changes in product selectivity.<sup>7</sup> Thus, fundamental knowledge of how these rearrangements occur may allow for enhanced control of substrate and product selectivity.

Although there are several ways to examine rearrangement mechanisms, one of the most convenient approaches involves deuterium labeling of the transition metal complex (catalyst) or substrate.<sup>8</sup> The product(s) of the resulting rearrangement can then be studied by techniques such as <sup>1</sup>H, <sup>2</sup>H, and/or <sup>13</sup>C{<sup>1</sup>H} NMR or IR spectroscopies, whereby insight into reactive C–H bonds is afforded by the “scrambling” of deuterium for hydrogen nuclei. Therefore, the results of deuterium labeling, spectroscopic studies, and some kinetic experiments have been used to elucidate the general mechanism of the rearrangements reported here. This appears to involve both intramolecular aromatic and aliphatic C–H bond activation coupled with the rupture and formation of Ru–C and Ru–N bonds.

## Results

### Synthesis of the New Ru(II) Complexes of NCN.

The synthetic strategy involved in the synthesis of the target complexes  $[RuCl\{C_6H_3(CH_2NMe_2)_{2-2,6-C,N}\}(\eta^6-C_{10}H_{14})]$  (**2**;  $C_{10}H_{14}$  = *p*-cymene = C<sub>6</sub>H<sub>4</sub>Me-<sup>*i*</sup>-Pr-4) and  $[Ru\{C_6H_3(CH_2NMe_2)_{2-2,6-C,N}\}(\eta^5-C_5H_5)(PPh_3)]$  (**5**) is based on the transmetalation of  $[Li\{C_6H_3(CH_2NMe_2)_{2-2,6}\}]_2$  (**1**) or  $[Na(C_5H_5)]_n$  ( $C_5H_5$  = Cp) with the known complexes  $[RuCl_2(\eta^6-C_{10}H_{14})]_2$  and  $[RuCl\{C_6H_3(CH_2NMe_2)_{2-2,6-N,C,N'}\}(PPh_3)]$  (**4**),<sup>3a</sup> respectively. This is depicted in Scheme 1. Transmetalation of an equimolar quantity of  $[RuCl_2(\eta^6-C_{10}H_{14})]_2$  in diethyl ether with **1**

(3) (a) Sutter, J.-P.; James, S. L.; Steenwinkel, P.; Karlen, T.; Grove, D. M.; Veldman, N.; Smeets, W. J. J.; Spek, A. L.; van Koten, G. *Organometallics* **1996**, *15*, 941. (b) Steenwinkel, P.; James, S. L.; Veldman, N.; Kooijman, H.; Spek, A. L.; Grove, D. M.; van Koten, G. *Chem. Eur. J.* **1996**, *2*, 1440.

(4) (a) Sutter, J.-P.; Grove, D. M.; Beley, M.; Collin, J.-P.; Veldman, N.; Spek, A. L.; Sauvage, J.-P.; van Koten, G. *Angew. Chem., Int. Ed. Engl.* **1994**, *33*, 1282. (b) Sutter, J.-P.; Beley, M.; Collin, J.-P.; Veldman, N.; Spek, A. L.; Sauvage, J.-P.; van Koten, G. *Mol. Cryst. Liq. Cryst.* **1994**, *253*, 215. (c) Steenwinkel, P.; Grove, D. M.; Veldman, N.; Spek, A. L.; van Koten, G. *Organometallics*, submitted.

(5) For hydrogen-transfer catalysis by ruthenium complexes of NCN and the related PCP ligand (PCP =  $[C_6H_3(CH_2PPh_2)_{2-2,6}]^-$ ) see: (a) Jiang, Q.; van Plew, D.; Murtuza, S.; Zhang, X. *Tetrahedron Lett.* **1996**, *37*, 797, and references therein. (b) Dani, P.; Karlen, T.; Gossage, R. A.; Steenwinkel, P.; van Koten, G. Manuscript in preparation. (c) Steenwinkel, P.; Gossage, R. A.; van Koten, G. *Chem. Eur. J.* **1998**, *4*, 759.

(6) (a) Cramer, R.; Lindsey, R. V. *J. Am. Chem. Soc.* **1966**, *88*, 3534. (b) Whetten, R. L.; Fu, K.-J.; Grant, E. R. *Ibid.* **1982**, *104*, 4270. (c) Emerson, G. F.; Pettit, R. *Ibid.* **1962**, *84*, 4591. (d) Bishop, K. C. *Chem. Rev.* **1976**, *76*, 461. (e) Iranpoor, N.; Mottaghinejad, E. *J. Organomet. Chem.* **1992**, *423*, 399. (f) Blanco, L.; Helson, H. E.; Hirthammer, M.; Mesdagh, H.; Spyroudis, S.; Vollhardt, K. P. C. *Angew. Chem., Int. Ed. Engl.* **1987**, *26*, 1246. (g) Maitlis, P. M. *The Organic Chemistry of Palladium*, Vol. 2; Academic Press: New York. (h) Noyori, R.; Umeda, I.; Kawachi, H.; Takaya, H. *J. Am. Chem. Soc.* **1975**, *97*, 812.

(7) (a) Kravchenko, R.; Masood, A.; Waymouth, R. M. *Organometallics* **1997**, *16*, 3635. (b) Coates, G. W.; Waymouth, R. M. *Science* **1995**, *267*, 217. (c) Brintzinger, H. H.; Fischer, D.; Mülhaupt, R.; Rieger, B.; Waymouth, R. M. *Angew. Chem., Int. Ed. Engl.* **1995**, *34*, 1143. (d) Möhring, P. C.; Coville, N. J. *J. Organomet. Chem.* **1994**, *479*, 1. (e) Gilchrist, J. H.; Bercaw, J. E. *J. Am. Chem. Soc.* **1997**, *119*, 12021. (f) Herzog, T. A.; Zubris, D. L.; Bercaw, J. E. *Ibid.* **1997**, *119*, 11988.

(8) (a) van der Zeijden, A. A. H.; van Koten, G.; Luijk, R.; Norde-mann, A.; Spek, A. L. *Organometallics* **1988**, *7*, 1549. (b) Rietveld, M. H. P.; Klumbers, E. G.; Jastrzebski, J. T. B. H.; Grove, D. M.; Veldman, N.; Spek, A. L.; van Koten, G. *Ibid.* **1997**, *16*, 4260.

at room temperature (RT) affords a red-brown suspension from which the novel complex **2** can be isolated in good yield. Complex **2** is moderately soluble in C<sub>6</sub>H<sub>6</sub>, tetrahydrofuran (THF), and chlorinated solvents, sparingly soluble in Et<sub>2</sub>O, and insoluble in alkanes. Analytically pure samples of this complex (large orange needles) were obtained by slow diffusion of pentane into a THF solution of **2**. This procedure afforded crystals that were also suitable for an X-ray structure analysis (vide infra). It should be noted that attempts at related transmetalation of [Li(C<sub>6</sub>H<sub>4</sub>(CH<sub>2</sub>NMe<sub>2</sub>)-2)]<sub>4</sub> (i.e., [Li<sub>4</sub>(dmba)<sub>4</sub>]) with arene Ru(II) complexes lead only to the formation of metallic Ru.<sup>9a-c</sup>

Treatment of a THF solution of **4**<sup>3a</sup> with a THF solution of [NaCp]<sub>n</sub> (Scheme 1) results in a yellow-brown mixture, from which yellow complex **5** was isolated in 75% yield. Compound **5** is moderately soluble in THF, C<sub>6</sub>H<sub>6</sub>, and toluene, sparingly soluble in Et<sub>2</sub>O, and insoluble in alkane solvents. Recrystallization of **5** from a mixture of C<sub>6</sub>H<sub>6</sub> and pentane afforded analytically pure, orange crystals that were also suitable for an X-ray analysis (vide infra). Complexes **2** and **5** are both air-stable in the solid state, but are sensitive to air in solution.

**Solution Spectroscopy of 2 and 5.** Complexes **2** and **5** have been characterized in solution by <sup>1</sup>H and <sup>13</sup>C NMR spectroscopy, and these spectra afford resonances consistent with diamagnetic Ru(II) complexes having low molecular symmetry (Scheme 1). Resonance values are typical for the organic fragments that are found in these compounds. The NMR data for all the new complexes reported herein can be found in Table 1.

The <sup>1</sup>H NMR spectrum (RT, C<sub>6</sub>D<sub>6</sub>) of **2** contains aromatic proton signals of the coordinated *p*-cymene unit which appear as four slightly broadened doublet resonances. These resonances become sharper upon raising the temperature to 320 K and at lower temperature (244 K; toluene-*d*<sub>8</sub>) broaden further with loss of their doublet structure and begin to show decoalescence behavior ( $\omega_{1/2} > 20$  Hz). This temperature-dependent behavior is probably due to restricted rotation of the *p*-cymene ligand, whereby a number of preferred rotamers can be envisioned at low temperature.<sup>10</sup> The <sup>13</sup>C-{<sup>1</sup>H} NMR spectrum of **2** (RT) contains 21 resonances. Four of the aromatic signals are broad, and these are assigned to the aromatic C-H carbon atoms of the coordinated *p*-cymene group.

The <sup>1</sup>H NMR spectrum of **5** (RT, C<sub>6</sub>D<sub>6</sub>), unlike that of **2**, shows no temperature-dependent solution behavior. The <sup>13</sup>C-{<sup>1</sup>H} NMR spectrum of **5** also reflects the asymmetric nature of this complex and contains 16 resonances. The resonance of Ru-C<sub>ipso</sub> of the NCN ligand and that of one methyl group of the coordinated NMe<sub>2</sub> group show coupling to phosphorus (<sup>2</sup>J<sub>PC</sub> = 16 Hz and <sup>3</sup>J<sub>PC</sub> = 4 Hz, respectively; Table 1).

It is worthwhile remarking that in complex **4** the

NCN ligand provides meridional  $\eta^3$ -*N,C,N'* bonding to the metal center.<sup>3a</sup> However, **2**, which is formally related to **4** by replacement of the PPh<sub>3</sub> by the neutral *p*-cymene ligand, contains an NCN ligand in a *C,N*-bidentate bonding mode. The same change of  $\eta^3$ - to  $\eta^2$ -bonding is found when the chloride ligand in **4** is replaced by an  $\eta^5$ -bonded Cp fragment (**5**). In **2** and **5**, the preferred formal 18-electron count of the metal center is achieved without coordination of another (sterically bulky) *ortho*-CH<sub>2</sub>NMe<sub>2</sub> substituent (see Discussion). In this sense, complexes **2** and **5** can be seen as analogues of complexes containing the dmba ligand with an *ortho* aromatic H having been replaced by a -CH<sub>2</sub>NMe<sub>2</sub> group.

**Synthesis of a 1,4-Phenylene-Bridged Bisruthenium(II) Complex.** To synthesize 1,4-phenylene-bridged bimetallic complexes, we recently developed a synthetic protocol which was applied to the preparation of a series of dinuclear organometallic complexes of the C<sub>2</sub>N<sub>4</sub> ligand.<sup>2</sup> Adapting this methodology here led to the following reaction sequence. The addition of 2.5 equiv of *n*-BuLi to an Et<sub>2</sub>O solution of C<sub>6</sub>Br<sub>2</sub>(CH<sub>2</sub>NMe<sub>2</sub>)<sub>4-2,3,5,6</sub> (**7**) results in the in situ formation of the polymeric reagent [1,4-Li<sub>2</sub>{C<sub>6</sub>(CH<sub>2</sub>NMe<sub>2</sub>)<sub>4-2,3,5,6</sub>}]<sub>n</sub> (**8**), which separates quantitatively from the solution as a white solid.<sup>2b</sup> Treatment of this material, resuspended in THF, with an equimolar quantity (metal-to-metal) of [RuCl<sub>2</sub>( $\eta^6$ -C<sub>10</sub>H<sub>14</sub>)]<sub>2</sub> affords the bimetallic complex **9**, which has been isolated as an orange-brown solid in moderate yield. The presence of residual C<sub>6</sub>H<sub>2</sub>(CH<sub>2</sub>NMe<sub>2</sub>)<sub>4-2,3,5,6</sub> and [RuCl<sub>2</sub>( $\eta^6$ -C<sub>10</sub>H<sub>14</sub>)]<sub>2</sub> in the reaction mixture suggests that partial hydrolysis of **8** by traces of water has occurred. Complex **9** is slightly soluble in chlorinated solvents and THF, but is insoluble in alkane and aromatic solvents. The poor solubility of **9** together with its air sensitivity in solution has precluded its successful recrystallization and purification from the residual starting materials. However, the crude product has been characterized in solution by <sup>1</sup>H NMR spectroscopy. The available evidence indicates that **9** is a complex in which the two metal coordination spheres are symmetry related and bridged by the C<sub>2</sub>N<sub>4</sub> ligand, as illustrated in Scheme 2. The <sup>1</sup>H NMR spectrum of **9** (RT, CDCl<sub>3</sub>) provides resonance patterns that show that the C<sub>2</sub>N<sub>4</sub> ligand has, like NCN in **2** and **5**, both coordinated and noncoordinated CH<sub>2</sub>NMe<sub>2</sub> units (Table 1). The *p*-cymene ligand affords four slightly broadened doublet resonances assigned to the aryl ring protons. As was observed for **5**, these latter resonances become sharp at higher temperature (320 K).

#### Thermal Rearrangement Reactions of 2 and 5.

It was observed that a <sup>1</sup>H NMR spectrum of complex **2** (CDCl<sub>3</sub>) that had been left standing (RT; 3 days) was significantly different from that of a freshly prepared sample. The <sup>1</sup>H NMR spectrum of the "aged" sample contained resonances of free protonated NCN (i.e., C<sub>6</sub>H<sub>4</sub>(CH<sub>2</sub>NMe<sub>2</sub>)<sub>2-1,3</sub> from some decomposition) and a resonance pattern that appeared to belong to a different organometallic compound. Subsequent studies in various solvents showed that complex **2** is thermally unstable in solution. In C<sub>6</sub>H<sub>6</sub> solution at 80 °C, **2** converts into this new species with minimal decomposition and isolated material from these reactions has been characterized as [RuCl{C<sub>6</sub>H<sub>3</sub>(CH<sub>2</sub>NMe<sub>2</sub>)<sub>2-2,4-C,N'</sub>}( $\eta^6$ -C<sub>10</sub>H<sub>14</sub>)]

(9) (a) Abbenhuis, H. C. L.; Pfeffer, M.; Sutter, J.-P.; de Cian, A.; Fischer, J.; Li Ji, H.; Nelson, J. H. *Organometallics* **1993**, *12*, 4464. (b) Attar, S.; Catalano, V. J.; Nelson, J. H. *Ibid.* **1996**, *15*, 2932. (c) Attar, S.; Nelson, J. H.; Fischer, J.; de Cian, A.; Sutter, J.-P.; Pfeffer, M. *Ibid.* **1995**, *14*, 4559. (d) Vicente, J.; Saura-Llamas, I.; Palin, M. G.; Jones, P. G.; Ramirez de Arellano, M. C. *Ibid.* **1997**, *16*, 826. (e) Pfeffer, M.; Sutter, J.-P.; Urriolabeitia, E. P. *Inorg. Chim. Acta* **1996**, *249*, 63.

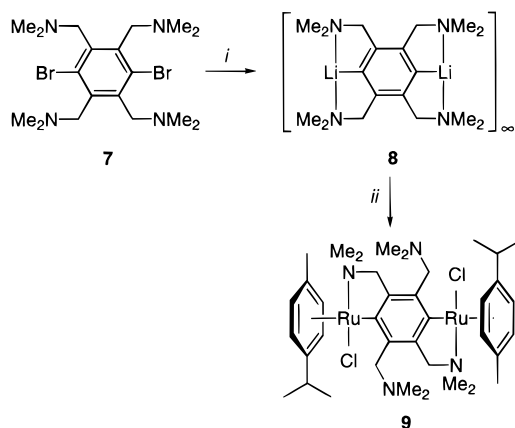
(10) McGlinchey, M. *Adv. Organomet. Chem.* **1992**, *34*, 285.



**Table 1. NMR Data for Complexes 2, 3, 5, 6, 2-*d*<sub>3</sub>, 3-*d*<sub>3</sub>, 4-*d*<sub>3</sub>, 5-*d*<sub>3</sub>, 6-*d*<sub>3</sub>, and 9<sup>a</sup>**

complex	<sup>1</sup> H				<sup>13</sup> C{ <sup>1</sup> H}			
	phenyl	<i>p</i> -cymene	NCH <sub>2</sub>	NCH <sub>3</sub>	phenyl	<i>p</i> -cymene	NCH <sub>2</sub>	NCH <sub>3</sub>
<b>2</b>	7.49 (d, 7.5)	6.00 (d, 4.0)	4.39 (d, 12.2)	2.48	176.1, 147.5	110.9, <sup>b</sup> 95.1 <sup>b</sup>	77.0	56.6
	7.06 (t, 7.4)	5.53 (d, 3.2)	3.42 (d, 12.2)	2.38	129.7, 122.2	86.9, <sup>b</sup> 84.5 <sup>b</sup>	66.7	51.8
	6.87 (d, 7.1)	4.38 (d, 5.0)	3.40 (d, 12.3)	1.95	120.8	80.0, 78.1		45.6
		3.93 (d, 5.6)	2.90 (d, 12.3)			30.9, 24.5		
		2.80 (s, 6.8)				20.2, 17.9		
<b>3</b>		1.59						
		1.14 (d, 6.8)						
		1.04 (d, 6.8)						
	8.08 (d, 11.4)	4.93 (d, 5.7)	4.51 (d, 12.5)	2.73	168.1, 147.2	109.7, 93.9	71.4	56.9
	7.37 (d, 7.5)	4.80 (d, 5.8)	3.46	2.21	138.2, 133.8	87.7, 86.4	65.1	54.5
	7.09	4.09 (d, 5.9)	2.41 (d, 12.5)	1.99	126.9, 122.6	80.4, 77.6		45.7
		3.89 (d, 5.6)				30.5, 23.1		
		2.85 (s, 6.9)				21.3, 17.7		
		1.72						
		1.13 (d, 6.9)						
		0.90 (d, 7.0)						
complex	<sup>1</sup> H				<sup>13</sup> C{ <sup>1</sup> H}			
	phenyl	C <sub>5</sub> H <sub>5</sub>	NCH <sub>2</sub>	NCH <sub>3</sub>	phenyl	C <sub>5</sub> H <sub>5</sub>	NCH <sub>2</sub>	NCH <sub>3</sub>
<b>5<sup>c</sup></b>	7.74 (7.3)	4.33	3.51 (13.3)	2.28	175.4 (16 <sup>d</sup> )	78.5 (2 <sup>d</sup> )	81.2	59.3
	7.26 (7.3)		3.30 (13.3)	2.21	149.5, 148.7		70.2	57.0
			3.34 (12.7)	1.82	125.8, 120.8			46.0
			2.69 (12.7)		120.1			
<b>6<sup>e</sup></b>	8.11 (7.5, 1.2)	4.18	3.47	2.48	170.3 (19 <sup>d</sup> )	79.4 (2 <sup>d</sup> )	73.9	60.2
	7.19 (7.4)		2.44 (13.4)	2.26	148.6, 142.6		65.3	59.4
	6.97		2.36 (13.4)	2.24	130.8, 126.0			45.6
					122.6			
complex	<sup>1</sup> H				<sup>13</sup> C{ <sup>1</sup> H}			
	phenyl	<i>p</i> -cymene	NCH <sub>2</sub>	NCH <sub>3</sub>	phenyl	<i>p</i> -cymene	NCH <sub>2</sub>	NCH <sub>3</sub>
<b>2-<i>d</i><sub>3</sub><sup>f</sup></b>	n.o.	6.03 (5.2)	4.39 (12.2)	2.48	176.5, 147.5	110.9, 95.1	76.9	56.7
		5.54 (4.9)	3.41 (12.2)	2.38	144.4, 129.6	86.9, 84.5	66.7	51.9
		4.38 (5.0)	3.35 (12.2)	1.96	121.9, 120.7	80.0, 78.1		45.7
		3.93 (5.6)	2.90 (12.2)			30.9, 24.5		
		2.80 (6.8)				20.2, 17.9		
		1.60						
<b>3-<i>d</i><sub>3</sub><sup>g</sup></b>		1.14 (6.8)						
		1.04 (6.8)						
	7.09	4.95 (5.7)	4.51 (12.6)	2.71	168.0, 147.2	109.7, 93.9	71.4	56.9
		4.81 (5.9)	3.47	2.21	138.1, 133.6	87.6, 86.4	65.0	54.5 <sup>h</sup>
		4.10 (5.9)	2.42 (12.6)	1.99	126.8, 122.6	80.4, 77.6		45.7
<b>4-<i>d</i><sub>3</sub><sup>i</sup></b>		3.91 (5.7)				30.5, 23.1		
			2.94 (13.8)	2.31	186.0 (15 <sup>d</sup> )		74.2	52.9
			2.71 (13.8)	2.18	148.6, 120.0 <sup>j</sup>			48.6
complex	<sup>1</sup> H				<sup>13</sup> C{ <sup>1</sup> H}			
	phenyl	C <sub>5</sub> H <sub>5</sub>	NH <sub>2</sub>	NCH <sub>3</sub>	phenyl	C <sub>5</sub> H <sub>5</sub>	NCH <sub>2</sub>	NCH <sub>3</sub>
<b>5-<i>d</i><sub>3</sub><sup>k</sup></b>	n.o.	4.33	3.51 (13.4)	2.29	175.3 (17 <sup>d</sup> )	78.5 (2 <sup>d</sup> )	78.6	59.3
			3.33 (12.7)	2.21	149.4, 148.6		70.2	57.0 (4 <sup>d</sup> )
			3.30 (13.4)	1.82				46.0
			2.69 (12.7)					
<b>6-<i>d</i><sub>3</sub><sup>l</sup></b>	7.18	4.18	3.46	2.50	170.2 (19 <sup>d</sup> )	79.4 (2 <sup>d</sup> )	73.9	60.2
	6.96		2.43 (13.6)	2.25	148.6, 130.7		65.3	59.4
			2.35 (13.6)	2.23	125.7, 122.6		60.2	45.7
complex	<sup>1</sup> H				<sup>13</sup> C{ <sup>1</sup> H}			
	phenyl	<i>p</i> -cymene	NCH <sub>2</sub>	NCH <sub>3</sub>	phenyl	C <sub>5</sub> H <sub>5</sub>	NCH <sub>2</sub>	NCH <sub>3</sub>
<b>9<sup>m</sup></b>		5.48 (5.4)	3.85 (13.8)	3.23				
		5.18 (5.6)	3.58–3.30 (m)	2.17				
		4.50 (5.5)		2.11				
		4.35 (5.5)						
		2.66 (7.0)						
		1.60						
		1.13 (7.0)						
		1.08 (6.7)						

<sup>a</sup> All NMR spectra were recorded in benzene-*d*<sub>6</sub> at ambient temperature unless otherwise noted. Chemical shifts are in ppm from the appropriate standards, and coupling constants are in hertz. All signals are singlets except where noted. Phenyl resonances are those of the NCN' ligand only. br = broad; d = doublet or AB pattern; dd = doublet of doublets; m = multiplet; s = septet. <sup>b</sup> Broad signal. <sup>c</sup> PPh<sub>3</sub> resonances:  $\delta_H$  = 7.44 (m), 7.02 (m);  $\delta_C$  = 141.0 (d, *J* = 32), 134.3 (d, *J* = 11), 128.7 (d, *J* = 2), 128.6;  $\delta_P$  = 53.4. <sup>d</sup> *J*<sub>CP</sub>. <sup>e</sup> PPh<sub>3</sub> resonances:  $\delta_H$  = 8.11 (dd, *J* = 7.5, 1.2), 7.56 (m), 7.04 (m);  $\delta_C$  = 140.7 (d, *J* = 34), 134.4 (d, *J* = 11), 130.8, 128.7 (d, *J* = 1), 127.5 (d, *J* = 10);  $\delta_P$  = 56.1. <sup>f</sup>  $\delta_D$  = 7.5–6.5 (br, m). <sup>g</sup>  $\delta_D$  = 7.90 (br), 7.5–6.5 (br, m), 2.6 and 1.9 (br, NCH<sub>2</sub>D). <sup>h</sup> A small triplet is also visible with *J*<sub>CD</sub> = 14 and 15 Hz, respectively for NCH<sub>2</sub>D. <sup>i</sup> PPh<sub>3</sub> resonances:  $\delta_H$  = 7.59 (m), 7.22 (m), 6.95 (t);  $\delta_C$  = 136.7 (d, *J* = 47), 134.5 (d, *J* = 10), 128.8 (d, *J* = 2), 127.2 (d, *J* = 10);  $\delta_P$  = 90.2. <sup>j</sup> Multiplet signal; *J*<sub>CD</sub> not resolved. <sup>k</sup>  $\delta_D$  = 7.5–6.5 (br, m). PPh<sub>3</sub> resonances:  $\delta_H$  = 7.45 (m), 7.01 (m);  $\delta_C$  = 141.0 (d, *J* = 32), 134.3 (d, *J* = 11), 128.7 (d, *J* = 2), 128.6;  $\delta_P$  = 53.9. <sup>l</sup>  $\delta_D$  = 8.0 (br), 6.0 (br), 2.1 (br, NCH<sub>2</sub>D). PPh<sub>3</sub> resonances:  $\delta_H$  = 7.55 (m), 7.03 (m);  $\delta_C$  = 140.7 (d, *J* = 34), 134.4 (d, *J* = 11), 128.7, 128.6 (d, *J* = 10);  $\delta_P$  = 56.1. <sup>m</sup> Recorded in CDCl<sub>3</sub>.

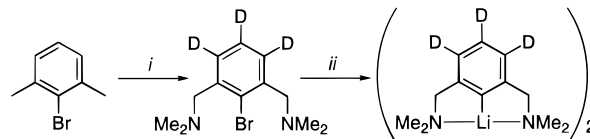
**Scheme 2. Synthesis of Complex 9<sup>a</sup>**

<sup>a</sup> Conditions: (i)  $2.5 \times n\text{-BuLi}$ ,  $\text{Et}_2\text{O}$ ,  $-78^\circ\text{C} \rightarrow \text{RT}$ , centrifugation; (ii) 1 equiv  $[\text{RuCl}_2(\eta^6\text{-C}_{10}\text{H}_{14})]_2$ , THF, RT.

(**3**), which is an isomer of **2**. Complex **3** can be obtained in up to 74% yield as orange air-stable crystals that are insoluble in  $\text{Et}_2\text{O}$  and THF and only moderately soluble in chlorinated solvents or  $\text{C}_6\text{H}_6$ . Compound **3** was further characterized by  $^1\text{H}$  and  $^{13}\text{C}\{^1\text{H}\}$  NMR spectroscopy and shows resonance patterns significantly shifted from those of **2** (Table 1). In addition, the aromatic proton resonances of the  $\eta^6$ -arene fragment are sharp at RT. To confidently characterize **3**, we have also attempted the preparation of this new product by an independent synthesis that involves the direct cyclo-metalation of 1,3-bis[(dimethylamino)methyl]benzene with  $[\text{RuCl}_2(\eta^6\text{-C}_{10}\text{H}_{14})]_2$  in the presence of  $\text{NaPF}_6$  (see Scheme 1 and the Experimental Section).<sup>1c,9a</sup> Carrying out this procedure in  $\text{CH}_2\text{Cl}_2$  solution yields exclusively **3**. Unfortunately, the yield by this route was only 27% after column chromatography (silica gel,  $\text{CH}_2\text{Cl}_2$  as elutant) and recrystallization. Crystals of **3** (orange needles), which were suitable for an X-ray analysis, were obtained by slow evaporation of a saturated solution of **3** in  $\text{MeOH}/\text{CH}_2\text{Cl}_2$  (1:1 v/v) under a stream of nitrogen gas.

The rate of the rearrangement reaction of **2** to **3** has been found to be solvent dependent. In  $\text{CDCl}_3$  solution (RT), the conversion of **2** to **3** is slow, whereas in  $\text{C}_6\text{H}_6$  or toluene there is no evidence for the formation of **3** after 72 h at ambient temperatures. The latter property enables one to study the onset temperature for the rearrangement of complex **2** to **3** in toluene- $d_8$  and to monitor this process by  $^1\text{H}$  NMR spectroscopy. Starting at 295 K, a toluene- $d_8$  solution of **2** was warmed at a rate of  $40\text{ K h}^{-1}$ . Only resonances of complex **2** were observed up to a temperature of 345 K. At 355 K, resonances of **3** started to appear, and the temperature was then held constant. After maintaining this temperature for 3 h, no resonances of **2** remained and the only other resonances were those of **3** and a small amount (<10%) of  $[\text{C}_6\text{H}_4(\text{CH}_2\text{NMe}_2)_2\text{-1,3}]$  (i.e., free NCN-H).

The thermal stability of **5** has also been studied. It was found that a solution of **5** in  $\text{C}_6\text{D}_6$  when heated at reflux temperature in an NMR tube cleanly afforded a new stable organometallic species, **6**, with no indications of decomposition. The data that was obtained enabled the characterization of **6** as  $[\text{Ru}(\eta^5\text{-Cp})\{\text{C}_6\text{H}_3(\text{CH}_2\text{NMe}_2)_2\text{-2,4-}C,N\}(\text{PPh}_3)]$  (Scheme 1), which is an isomer of **5**.

**Scheme 3. Synthesis of the Deuterated Organolithium NCN Reagent  $[\text{Li}\{\text{C}_6\text{D}_3(\text{CH}_2\text{NMe}_2)_2\text{-2,6}\}]_2^a$** 

<sup>a</sup> Conditions: (i)  $\text{D}_2\text{SO}_4$ ,  $\text{D}_2\text{O}$ , reflux; NBS,  $\text{MeOAc}$ ,  $h\nu$ ;  $\text{HNMe}_2$ ,  $\text{Et}_2\text{O}$ ,  $0^\circ\text{C}$ ; (ii)  $t\text{-BuLi}$ ,  $\text{Et}_2\text{O}$ , or THF,  $-78^\circ\text{C} \rightarrow \text{RT}$ .

Compound **6**, a yellow solid, can be synthesized on a preparative scale by heating a solution of **5** in  $\text{C}_6\text{H}_6$  at reflux temperature for 2.5 h. Analytically pure yellow crystals of **6**, which were suitable for an X-ray analysis, were obtained by cooling ( $-10^\circ\text{C}$ ) a saturated solution of **6** in a mixture of pentane and  $\text{C}_6\text{H}_6$  (9:1 v/v). The  $^1\text{H}$  NMR resonances of **6** are shifted significantly relative to those of **5** (Table 1).

The thermal stability of **9** was likewise investigated. A solution of **9** (3 days, RT,  $\text{CDCl}_3$ ) afforded a  $^1\text{H}$  NMR spectrum that was similar to that of a freshly prepared sample, although there are traces (<10%) of free tetramine ( $[\text{C}_6\text{H}_2\{\text{CH}_2\text{NMe}_2\}_4\text{-1,2,4,5}]$ ). This result indicates that **9** is relatively stable under the reaction conditions that induce a facile 2,6- to 2,4-rearrangement of **2** and **5** (see Discussion). During all studies of the thermal rearrangement of **2** to **3** and **5** to **6**, there was no evidence for any reaction intermediates ( $^1\text{H}$  NMR spectroscopy) or, in the case of **5**, free  $\text{PPh}_3$ .

**Synthesis of Deuterium-Labeled Materials.** To investigate the mechanism of the thermal rearrangement of **2** and **5** more closely, complexes containing a deuterium-labeled derivative of the NCN ligand, i.e.,  $[\text{C}_6\text{D}_3(\text{CH}_2\text{NMe}_2)_2\text{-2,6}]^-$  (NCN- $d_3$ ), were synthesized. The synthetic route to complexes **2-*d*<sub>3</sub>** and **5-*d*<sub>3</sub>**, (i.e., analogues of **2** and **5** containing NCN- $d_3$ ) is similar to that shown in Scheme 1. This was accomplished by synthesizing the appropriate deuterium-labeled ligand precursor via the repeated treatment of 1-bromo-2,6-xylene with a mixture of  $\text{D}_2\text{O}$  and  $\text{D}_2\text{SO}_4$  (see Experimental Section) to afford 2,6-( $\text{CH}_3$ ) $_2\text{C}_6\text{D}_3\text{Br}$ ; see Scheme 3. This was followed by procedures that were analogous to those used in the synthesis of NCN-H.

As expected,  $^1\text{H}$  NMR spectra of complexes **2-*d*<sub>3</sub>** and **5-*d*<sub>3</sub>** are similar to those of their nondeuterated analogues, except for the expected low-intensity aromatic proton resonances of the NCN- $d_3$  ligand (Table 1). The corresponding  $^{13}\text{C}\{^1\text{H}\}$  NMR spectra were also similar to those of their nondeuterated analogues, but had much lower relative intensity for the  $\text{C}_{\text{aryl}}\text{-H}$  carbon atoms. Unfortunately, the low solubility of these materials prevents the observation of the characteristic equal intensity triplet resonances for the  $\text{C}_{\text{aryl}}\text{-D}$  carbon atoms (coupling with deuterium;  $I = 1$ ). Furthermore, the incorporation of deuterium in the aromatic ring of NCN- $d_3$  could be unambiguously confirmed by  $^2\text{H}$  NMR spectra of complexes **2-*d*<sub>3</sub>** and **5-*d*<sub>3</sub>**. These spectra showed resonances only in the region of 6.5–8 ppm.

**Mechanistic Studies.** A number of solution studies have been performed to obtain insight into the mechanism(s) involved in the rearrangement of **2** and **5** to **3** and **6**, respectively. First, the examination of possible solvent effects was carried out to determine whether the

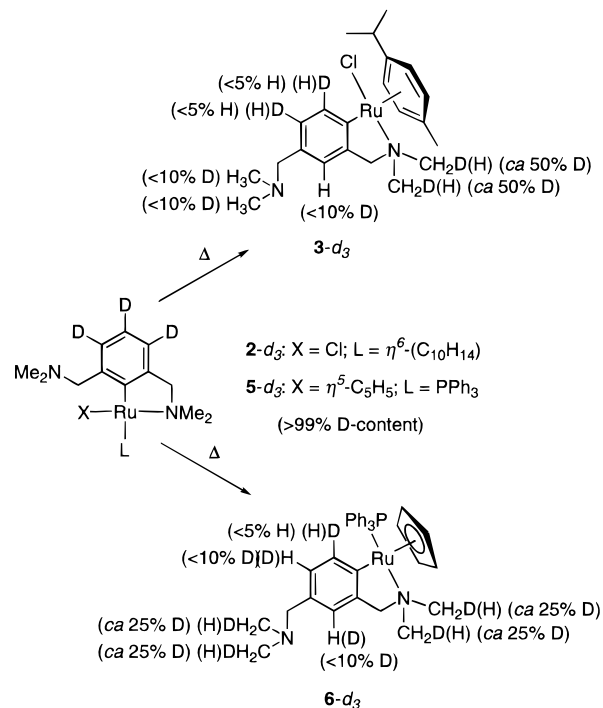
medium was participating in the overall isomerization. This was accomplished by comparing the products from the rearrangement reactions in deuterated and non-deuterated solvents. The  $^1\text{H}$  and  $^{13}\text{C}\{^1\text{H}\}$  NMR spectra of solutions of **2** and **5** in  $\text{C}_6\text{D}_6$ , which were heated at reflux temperature for 1 h, showed no evidence for deuterium incorporation in the resulting products **3** and **6**. Moreover, complete decomposition occurs when a solution of **2** ( $\text{C}_6\text{D}_6$ ) is heated at reflux temperature for 24 h. Addition of  $\text{CH}_2\text{Cl}_2$  followed by filtration of the residual mixture (a black insoluble residue was left behind) and analysis of the  $\text{C}_6\text{D}_6/\text{CH}_2\text{Cl}_2$  filtrate (via GC–MS and  $^1\text{H}$  NMR spectroscopy) showed the presence free  $\text{C}_{10}\text{H}_{14}$  and  $\text{C}_6\text{H}_4(\text{CH}_2\text{NMe}_2)_2$ -1,3. Neither of these organic compounds had significant deuterium incorporation. These results indicate that there is no solvent C–H(D) bond activation<sup>11</sup> at any stage of the isomerization of **2** to **3** or **5** to **6**.

In a second investigation, some limited concentration-dependent kinetic experiments were carried out to determine whether the rearrangements were either inter- and/or intramolecular processes. Benzene solutions of two different concentrations of complex **2** or **5** were prepared and heated to reflux temperatures (see Experimental Section). At appropriate time intervals, samples were taken from the homogeneous reaction solution, and these were evaporated to dryness and analyzed by  $^1\text{H}$  NMR spectroscopy ( $\text{C}_6\text{D}_6$ ). The intensities of the aromatic protons of the NCN ligand attached to complexes **2** and **3** were used to determine the relative concentrations of these complexes during the rearrangement process. Likewise, the relative concentrations of complexes **5** and **6** were calculated from the integration of the  $\text{C}_5\text{H}_5$  resonances (an internal standard was used for the calibration).

Although the conversion rates of the *p*-cymene complex **2** at concentrations of 10 and 48 mmol/L differed significantly ( $k = 1.35 \pm 0.1 \text{ s}^{-1}$  and  $2.74 \pm 0.2 \text{ s}^{-1}$ , respectively), this rearrangement was accompanied by a significant amount of decomposition (up to 50% in some runs) at complete conversion of **2**. This prevents us drawing any definitive conclusions regarding the nature of this rearrangement reaction. However, the rearrangement of complex **5** was found to exhibit pseudo-first-order kinetics ( $k_{\text{obs}} = 0.104 \pm 0.06 \text{ s}^{-1}$  and  $0.110 \pm 0.06 \text{ s}^{-1}$  at concentrations of 0.70 and 6.75 mmol/L, respectively). This result yields a calculated half-life of 6.5 min at 80 °C. This gives direct evidence that, within experimental error, the rearrangement reaction of complex **5** to its 2,4-isomer **6** is independent of the initial concentration of **5**. This strongly suggests that this rearrangement is an intramolecular, rather than intermolecular, process. By analogy, an intramolecular rearrangement can also be used to explain the conversion of **2** to **3**.

Complexes **2-d**<sub>3</sub> and **5-d**<sub>3</sub> were heated at reflux temperature in benzene for 2 h, and the resulting isomerized complexes **3-d**<sub>3</sub> and **6-d**<sub>3</sub> (Scheme 4) were subsequently examined by  $^1\text{H}$ ,  $^2\text{H}$ , and  $^{13}\text{C}\{^1\text{H}\}$  NMR spectroscopy to identify whether any deuterium scrambling had occurred from the aromatic ring of NCN-*d*<sub>3</sub> into other organic functionalities.

**Scheme 4. Deuterium Distribution upon Thermal Rearrangement of Complexes **2-d**<sub>3</sub> and **5-d**<sub>3</sub> to Complexes **3-d**<sub>3</sub> and **6-d**<sub>3</sub>, Respectively**



The  $^1\text{H}$  NMR spectrum of complex **2-d**<sub>3</sub> shows no significant aromatic resonances for the NCN-*d*<sub>3</sub> ligand. However, the  $^1\text{H}$  NMR spectrum of the rearranged product **3-d**<sub>3</sub> contains a single aromatic resonance (integrating for one proton), which by comparison with data for **3** can be assigned to a proton at position-3 of the aromatic ring of the NCN ligand, i.e., a  $[\text{Ru}\{\text{C}_6(\text{CH}_2\text{NMe}_2)_2$ -2,4-*D*<sub>2</sub>-5,6-*H*-3}] unit. Moreover, both methyl resonances of the coordinated  $\text{CH}_2\text{NMe}_2$  group show a shoulder peak, and the corresponding  $^{13}\text{C}\{^1\text{H}\}$  NMR resonances consist of a singlet resonance together with a small triplet arising from coupling with deuterium ( $^1J_{\text{CD}} = 14$  and 15 Hz). These data indicate the presence of deuterium in both methyl groups of the coordinated dimethylamino group in **3-d**<sub>3</sub>. The  $^{13}\text{C}\{^1\text{H}\}$  NMR spectrum of **3-d**<sub>3</sub> also shows a singlet resonance for the protonated C-3 carbon atom without a corresponding C–D triplet. Based on a signal-to-noise evaluation of this spectrum, this result puts an upper limit of 10% on possible deuterium incorporation at this position. A  $^2\text{H}$  NMR spectrum of **3-d**<sub>3</sub> shows not only a resonance in the aromatic region (integrating for two deuterium atoms) but also two resonances (each integrating for one-half of a deuterium atom) in the aliphatic region at shift positions corresponding to those of the methyl groups of the coordinated  $\text{CH}_2\text{NMe}_2$  substituents of **3**. In summary, this experiment shows that a deuterium atom of NCN-*d*<sub>3</sub> is shifted from aromatic position C-3 in **2-d**<sub>3</sub> to both methyl groups of the coordinated  $\text{CH}_2\text{NMe}_2$  group in **3-d**<sub>3</sub>, where it is equally scrambled over the two methyl groups (0.5  $^2\text{H}$  in each). The other two deuterium atoms appear to remain on the aromatic ring at their original positions (i.e., on C-4 and C-5 in **2-d**<sub>3</sub> and C-5 and C-6 in **3-d**<sub>3</sub>).

The  $^1\text{H}$  NMR spectrum of complex **6-d**<sub>3</sub> (the rearrangement product of **5-d**<sub>3</sub>) contains two new (singlet) resonances (integrating for two protons) in the aromatic

(11) Lenges, C. P.; Brookhart, M.; Grant, B. E. *J. Organomet. Chem.* **1997**, *528*, 199.



region. These protons are, by comparison with  $^1\text{H}$  NMR data of **6**, at positions C-3 and C-5. Therefore **6-d<sub>3</sub>** contains a  $[\text{Ru}\{\text{C}_6(\text{CH}_2\text{NMe}_2)_{2-2,4-D-6-H-3,5}\}]$  unit, i.e., the  $^2\text{H}$  atoms at positions 3 and 5 in **5-d<sub>3</sub>** have been replaced by protons during the rearrangement process. In the  $^{13}\text{C}\{^1\text{H}\}$  NMR spectrum of **6-d<sub>3</sub>**, the coordinated and the noncoordinated  $-\text{CH}_2\text{NMe}_2$  group together afford three methyl singlet resonances which all show a superimposed small triplet resonance; the latter is arising from coupling with deuterium ( $^1J_{\text{C-D}} = \text{ca. } 20 \text{ Hz}$ ). Unfortunately, the overlapping coupling with  $^{31}\text{P}$  prevented the exact determination of the coupling constants. In the aromatic region of this  $^{13}\text{C}$  NMR spectrum, there are two singlets (positions-3 and -5) and one equal intensity triplet corresponding to a C–D unit at position-6. The estimate of deuterium incorporation at positions-3 and -5 is less than 10%. The  $^2\text{H}$  NMR spectrum of **6-d<sub>3</sub>** shows, besides a resonance in the aromatic region (integrating for one deuterium atom), a broad resonance in the aliphatic region (integrating for two deuterium atoms). This is direct evidence for deuterium incorporation into the methyl groups of the  $\text{CH}_2\text{NMe}_2$  groups of the rearranged NCN ligand. In summary, two deuterium atoms of the NCN-d<sub>3</sub> ligand have shifted from aromatic positions C-3 and C-5 in **5-d<sub>3</sub>** into both the coordinated and the noncoordinated  $\text{CH}_2\text{NMe}_2$  substituents in **6-d<sub>3</sub>**, where they are equally scrambled (0.5  $^2\text{H}$ ). The third deuterium atom originally at aromatic position C-4 in **5-d<sub>3</sub>** remains fixed and hence becomes aromatic position C-6 in **6-d<sub>3</sub>**. The overall conclusion from these experiments using complexes **2-d<sub>3</sub>** and **5-d<sub>3</sub>** is that the intramolecular rearrangement processes involve activation of both aromatic and aliphatic C–H(D) bonds. The mechanistic proposals based on these results are detailed in the Discussion section.

The kinetics using both deuterated and nondeuterated materials have been compared to identify possible isotope effects. A solution of complex **5** and a solution of complex **5-d<sub>3</sub>** in  $\text{C}_6\text{D}_6$  were both heated at reflux temperature under identical conditions. After 5 and 8 min,  $^1\text{H}$  NMR spectra of both solutions were recorded to determine (by integration) the concentrations of **5** (-d<sub>3</sub>) and **6** (-d<sub>3</sub>). After these time intervals (41% conversion and 63% conversion, respectively), the rearrangement of both **5** and its deuterated analogue **5-d<sub>3</sub>** to **6** and **6-d<sub>3</sub>** was found to have proceeded at identical rates; that is, the kinetic isotope effect  $k_{\text{H}}/k_{\text{D}} = 1$ . From this one can conclude, in combination with the other results in this section, that the rate-determining step of the rearrangement reactions of **2** and **5** does not involve C–H(D) bond activation and may therefore involve initial rupture of a Ru–N bond.

**Solid-State Structures of 2, 3, 5 and 6.** To obtain more structural information on the new complexes in the solid state, X-ray crystallographic studies of these species have been performed. Table 2 contains selected geometrical parameters for the complexes **2** and **5** and their rearrangement products **3** and **6**. The molecular geometries of these complexes obtained from the crystallographic studies are illustrated in Figure 2–5. For the list of crystallographic data, see Table 3.

The molecular geometry of  $[\text{RuCl}\{\eta^2\text{-C}_6\text{H}_3(\text{CH}_2\text{NMe}_2)_{2-2,6-C,N}\}(\eta^6\text{-C}_{10}\text{H}_{14})]$ , **2**, shown in Figure 2, and its 2,4-

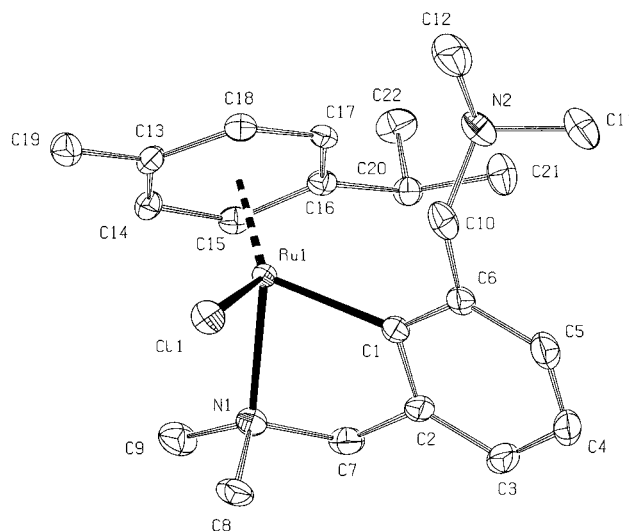


**Figure 2.** ORTEP drawing (50% probability atomic displacement ellipsoids) of the solid-state structure of  $[\text{RuCl}\{\eta^2\text{-C}_6\text{H}_3(\text{CH}_2\text{NMe}_2)_{2-2,6}\}(\eta^6\text{-C}_{10}\text{H}_{14})]$ , **2**. Hydrogen atoms have been omitted for clarity.

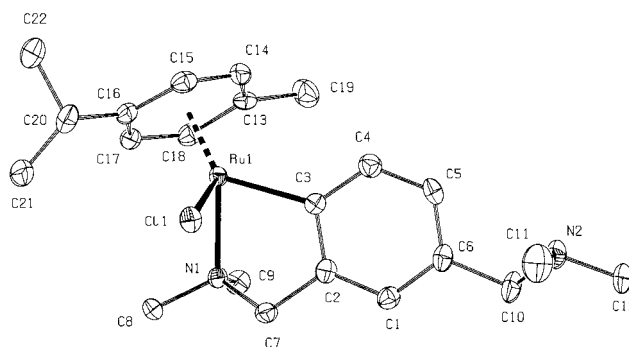


**Figure 3.** ORTEP drawing (50% probability atomic displacement ellipsoids) of the solid-state structure of  $[\text{RuCl}\{\eta^2\text{-C}_6\text{H}_3(\text{CH}_2\text{NMe}_2)_{2-2,4}\}(\eta^6\text{-C}_{10}\text{H}_{14})]$ , **3**. Hydrogen atoms have been omitted for clarity.

isomer **3** (Figure 3) reveal complexes in which the metal coordination sphere is composed of a chloride ligand, an  $\eta^6$ -bonded arene (*p*-cymene), and an NCN ligand that is coordinated in a *C,N*-bidentate fashion through an aromatic atom and an N-donor atom of a  $-\text{CH}_2\text{NMe}_2$  group. The metal center is in a distorted octahedral environment in both cases. The bidentate bonding of NCN affords a Ru–C bond distance of 2.075(4) Å (**2**) and 2.083(4) Å (**3**) and a Ru–N bond distance of 2.217(3) Å (**2**) and 2.203(4) Å (**3**). The ligand bite angle (C–Ru–N) is found to be 77.57(11)° in complex **2** and 77.98(13)° in **3**. A second  $\text{CH}_2\text{NMe}_2$  group of NCN is not coordinated to the metal center, and the lone pair of the N-donor atom appears to be oriented away from the metal. The aromatic ring of the NCN ligand is planar (deviations of the carbon atoms from the least-squares [LSQ] plane through the aromatic ring are less than  $\pm 0.006(4)$  Å in **2** and  $\pm 0.0014(4)$  Å in **3**) with only minor distortions of the C–C–C bond angles from 120°. The Ru center lies in the same plane (**2**,  $\angle\{\text{C–Ru}\}\{\text{LSQ}\} = 0.46(16)^\circ$ ; **3**,  $2.40(18)^\circ$ ). The bidentate *C,N*-coordination of NCN leads to a five-membered chelate ring that appears to be more strained in **2** than in **3**;

**Table 2.** Selected Bond Lengths and Angles of Complexes **2**, **3**, **5**, and **6**

bond distances (Å)		bond angles (deg)		dihedral angles (deg)	
2					
Ru(1)–C(1)	2.075(4)	C(1)–Ru(1)–N(1)	77.57(11)	C(1)–C(2)–C(3)–C(4)	–0.3(6)
Ru(1)–N(1)	2.217(3)	C(1)–C(2)–C(7)	116.2(3)	C(2)–C(3)–C(4)–C(5)	1.0(6)
Ru(1)–Cl(1)	2.4173(8)	C(3)–C(2)–C(7)	120.6(3)	C(3)–C(4)–C(5)–C(6)	–1.0(6)
Ru(1)–C(13)	2.293(3)	C(1)–C(2)–C(3)	123.2(3)	C(4)–C(5)–C(6)–C(1)	0.4(6)
Ru(1)–C(14)	2.287(3)	C(2)–C(3)–C(4)	118.8(3)	C(5)–C(6)–C(1)–C(2)	0.3(4)
Ru(1)–C(15)	2.170(3)	C(3)–C(4)–C(5)	119.3(3)	C(6)–C(1)–C(2)–C(3)	–0.3(5)
Ru(1)–C(16)	2.202(3)	C(4)–C(5)–C(6)	122.4(3)		
Ru(1)–C(17)	2.163(3)	C(5)–C(6)–C(1)	118.9(3)		
Ru(1)–C(18)	2.175(3)	C(6)–C(1)–C(2)	117.4(3)		
3					
Ru(1)–C(3)	2.083(4)	C(3)–Ru(1)–N(1)	77.98(13)	C(1)–C(2)–C(3)–C(4)	–1.6(6)
Ru(1)–N(1)	2.203(4)	C(1)–C(2)–C(7)	121.7(4)	C(2)–C(3)–C(4)–C(5)	2.5(6)
Ru(1)–Cl(1)	2.4279(13)	C(3)–C(2)–C(7)	116.2(4)	C(3)–C(4)–C(5)–C(6)	–1.1(7)
Ru(1)–C(13)	2.190(4)	C(1)–C(2)–C(3)	122.1(4)	C(4)–C(5)–C(6)–C(1)	–1.4(7)
Ru(1)–C(14)	2.165(4)	C(2)–C(3)–C(4)	115.9(4)	C(5)–C(6)–C(1)–C(2)	2.4(7)
Ru(1)–C(15)	2.170(4)	C(3)–C(4)–C(5)	122.8(4)	C(6)–C(1)–C(2)–C(3)	–0.8(7)
Ru(1)–C(16)	2.286(4)	C(4)–C(5)–C(6)	120.1(4)		
Ru(1)–C(17)	2.278(4)	C(5)–C(6)–C(1)	118.5(4)		
Ru(1)–C(18)	2.180(4)	C(6)–C(1)–C(2)	120.5(4)		
5					
Ru(1)–C(1)	2.071(5)	C(1)–Ru(1)–N(1)	78.05(19)	C(1)–C(2)–C(3)–C(4)	–1.6(10)
Ru(1)–N(1)	2.230(4)	C(1)–C(2)–C(7)	114.5(4)	C(2)–C(3)–C(4)–C(5)	0.9(10)
Ru(1)–P(1)	2.2897(15)	C(3)–C(2)–C(7)	121.7(5)	C(3)–C(4)–C(5)–C(6)	–0.2(11)
Ru(1)–C(13)	2.206(7)	C(1)–C(2)–C(3)	123.5(5)	C(4)–C(5)–C(6)–C(1)	0.0(2)
Ru(1)–C(14)	2.186(6)	C(2)–C(3)–C(4)	120.2(5)	C(5)–C(6)–C(1)–C(2)	–0.6(8)
Ru(1)–C(15)	2.187(5)	C(3)–C(4)–C(5)	118.8(5)	C(6)–C(1)–C(2)–C(3)	1.4(9)
Ru(1)–C(16)	2.222(5)	C(4)–C(5)–C(6)	121.3(5)		
Ru(1)–C(17)	2.234(6)	C(5)–C(6)–C(1)	121.5(5)		
		C(6)–C(1)–C(2)	114.7(4)		
6					
Ru(1)–C(3)	2.066(5)	C(3)–Ru(1)–N(1)	78.06(16)	C(1)–C(2)–C(3)–C(4)	1.0(7)
Ru(1)–N(1)	2.206(4)	C(1)–C(2)–C(7)	120.2(4)	C(2)–C(3)–C(4)–C(5)	–1.2(7)
Ru(1)–P(1)	2.2637(11)	C(3)–C(2)–C(7)	116.7(4)	C(3)–C(4)–C(5)–C(6)	1.0(7)
Ru(1)–C(13)	2.218(5)	C(1)–C(2)–C(3)	123.1(4)	C(4)–C(5)–C(6)–C(1)	–0.4(7)
Ru(1)–C(14)	2.161(5)	C(2)–C(3)–C(4)	114.5(4)	C(5)–C(6)–C(1)–C(2)	0.2(6)
Ru(1)–C(15)	2.193(5)	C(3)–C(4)–C(5)	122.1(5)	C(6)–C(1)–C(2)–C(3)	–0.5(7)
Ru(1)–C(16)	2.282(6)	C(4)–C(5)–C(6)	122.6(4)		
Ru(1)–C(17)	2.256(5)	C(5)–C(6)–C(1)	117.0(5)		
		C(6)–C(1)–C(2)	120.7(5)		

the  $sp^2$  carbon atom (C(1)) affords a Ru–C–C(2) bond angle of  $112.9(2)^\circ$  in **2**, while the corresponding angle in **3** is  $114.8(3)^\circ$ . As a consequence, the C atom positioned *para* to the Ru–C<sub>ipso</sub> bond provides a C<sub>para</sub>...C<sub>ipso</sub>–Ru angle of  $170.59(17)^\circ$  in **2** and  $172.5(2)^\circ$  in complex **3**. Another aspect of the chelate ring of **2** is the apparently unfavorable orientation of the N(1)–C(8) bond with respect to the Ru(1)–Cl(1) bond, which is virtually eclipsed (C(8)–N(1)–Ru(1)–Cl(1) dihedral angle =  $-11.5(2)^\circ$ ). The aromatic ring of the *p*-cymene ligand shows some small distortions from planarity; aromatic C–C bond angles vary from  $118.9(3)^\circ$  to  $122.8(3)^\circ$ , and dihedral angles in the ring vary from  $-6.1(5)^\circ$  to  $6.0(5)^\circ$ . One interesting aspect of the solid-state structure of **2** is the presence of short intramolecular separations between the aromatic *p*-cymene C–H unit C(17)–H(17) and the N(2) atom of the noncoordinated CH<sub>2</sub>NMe<sub>2</sub> group of the NCN ligand, i.e., 3.140(4) Å for C(17)···N(2) and 2.373(4) Å for H(17)···N(2). This point is addressed later in relation to solution behavior and the thermal rearrangements.

Finally, it is clear that in the solid-state structure of the rearranged isomer **3** that the *p*-cymene ligand does not interfere with the noncoordinated CH<sub>2</sub>NMe<sub>2</sub> group, which is now positioned *para* to the metal center. In complex **3**, the Ru(1)–Cl(1) bond is, unlike that in **2**, oriented in an energetically favorable way, being stag-

gered with respect to the N(1)–C(7) and N(1)–C(8) bonds, with dihedral angles of  $-57.6(2)^\circ$  and  $62.3(3)^\circ$ , respectively.

The solid-state molecular geometries of the 2,6-isomer **5** (Figure 4) and the 2,4-isomer (Figure 5) **6** clearly reveal the presence of a  $\eta^5$ -bonded Cp ligand, a *P*-coordinated triphenylphosphine ligand and an  $\eta^2$ -*C,N*-coordinated NCN unit, so affording the Ru centers with a distorted octahedral ligand array. The *C,N*-bidentate coordination of the NCN ligand through the aromatic ring via C(1) in **5** and C(3) in **6** and N(1) of one of the –CH<sub>2</sub>NMe<sub>2</sub> groups affords a five-membered chelate ring with Ru–C bond distances of 2.071(5) (5) and 2.066(5) Å (6) and Ru–N bond distances of 2.230(4) and 2.206(4) Å for **5** and **6**, respectively. The C–Ru–N bite angle is  $78.05(19)^\circ$  for **5**, with a similar value for **6** (Table 2). The Ru–C(cyclopentadiene) bond distances vary between 2.161(5) and 2.234(6) Å for both complexes. The Ru–P bond lengths (Table 2) are typical for Cp Ru(II) phosphine compounds.<sup>13</sup> The aromatic ring of the NCN ligand of **5** and **6** is, like that in **2** and **3**, planar with individual deviations of the ring carbon atoms from the LSQ plane through the aromatic ring of less than  $\pm 0.007(7)$  Å for **5** with a similar value for **6**. The Ru center lies in the same plane ( $\angle\{C(1)–Ru-$

(13) Bruce, M. I.; Wong, F. S.; Skelton, B. W.; White, A. H. *J. Chem. Soc., Dalton Trans.* **1981**, 1398.



**Table 3.** Crystallographic Data for **2**, **3**, **5**, and **6**

	<b>2</b>	<b>3</b>	<b>5</b>	<b>6</b>
Crystal Data				
formula	C <sub>22</sub> H <sub>33</sub> ClN <sub>2</sub> Ru	C <sub>22</sub> H <sub>33</sub> ClN <sub>2</sub> Ru	C <sub>35</sub> H <sub>39</sub> N <sub>2</sub> PRu	C <sub>35</sub> H <sub>39</sub> N <sub>2</sub> PRu
mol wt	462.04	462.04	619.75	619.75
cryst syst	orthorhombic	triclinic	monoclinic	monoclinic
space group	<i>Pbca</i> (No. 61)	<i>P</i> $\bar{1}$ (No. 2)	<i>C2/c</i> (No. 15)	<i>P2<sub>1</sub>/c</i> (No. 14)
<i>a</i> , Å	16.5185(13)	6.3649(7)	21.5618(4)	9.0383(12)
<i>b</i> , Å	14.4236(13)	12.4204(8)	17.012(2)	16.1222(14)
<i>c</i> , Å	17.8523(11)	14.2876(14)	18.941(2)	21.649(3)
$\alpha$ , deg		102.550(7)		
$\beta$ , deg		94.077(8)	121.285(6)	103.385(9)
$\gamma$ , deg		101.305(7)		
<i>V</i> , Å <sup>3</sup>	4253.4(6)	1073.47(18)	5937.5(11)	3068.9(7)
<i>D</i> <sub>calc</sub> , g cm <sup>-3</sup>	1.443	1.430	1.387	1.341
<i>Z</i>	8	2	8	4
<i>F</i> (000)	1920	480	2576	1288
$\mu$ [Mo K $\alpha$ ], cm <sup>-1</sup>	8.7	8.6	6.1	5.9
cryst size, mm	0.1 $\times$ 0.2 $\times$ 1.1	0.03 $\times$ 0.15 $\times$ 0.43	0.08 $\times$ 0.4 $\times$ 0.4	0.2 $\times$ 0.4 $\times$ 0.4
Data Collection				
$\theta_{\min}$ , $\theta_{\max}$ , deg	1.1, 27.5	1.5, 27.5	1.3, 27.5	1.0, 27.5
SET4 $\theta_{\min}$ , $\theta_{\max}$ , deg	11.42, 14.00 [25 refl]	10.01, 13.86 [25 refl]	11.45, 14.03 [25 refl]	11.66, 13.84 [23 refl]
$\Delta\omega$ , deg	0.74 + 0.35 tan $\theta$	0.80 + 0.35 tan $\theta$	0.71 + 0.35 tan $\theta$	1.25 + 0.35 tan $\theta$
hor., ver. aperture, mm	4.75 + 2.38 tan $\theta$ , 4.00	2.23 + 1.12 tan $\theta$ , 4.00	3.00 + 1.50 tan $\theta$ , 4.00	1.97 + 0.99 tan $\theta$ , 4.00
X-ray exposure time, h	16	21	26	25
linear decay, %	1	2	9	<1
reference reflns	4 2-2, 2 0-6, 2 5-2	2 1 4, 2-6-2, 2-1-6	-1-5-2, -1-5 2, 0, -4-4	-2 2-4, -3 2 4, 0-6-2
data set	-20:21, 0:18, -23:0	0:8, -16:15, -18:18	-28:23, 0:22, 0:24	-11:4, 0:20, -27:28
total data	9752	5369	16 392	7879
total unique data	4858	4923	6818	7007
<i>R</i> <sub>int</sub>	0.0253	0.0373	0.109 10	0.0183
Refinement				
no. of refined params	235	242	385	401
final <i>R</i> <sup>a</sup>	0.0377 [3411 <i>I</i> > 2 $\sigma$ ( <i>I</i> )]	0.0483 [3822 <i>I</i> > 2 $\sigma$ ( <i>I</i> )]	0.0532 [3814 <i>I</i> > 2 $\sigma$ ( <i>I</i> )]	0.0508 [5438 <i>I</i> > 2 $\sigma$ ( <i>I</i> )]
final w <i>R</i> <sup>2b</sup>	0.0768	0.0987	0.1305	0.1208
goodness of fit	1.031	1.030	0.994	1.183
<i>w</i> <sup>-1c</sup>	$\sigma^2(F^2) + (0.0201P)^2 + 0.08P$	$\sigma^2(F^2) + (0.0347P)^2 + 0.05P$	$\sigma^2(F^2) + (0.0507P)^2$	$\sigma^2(F^2) + (0.0225P)^2 + 11.84P$
( $\Delta/\sigma$ ) <sub>av</sub> , ( $\Delta/\sigma$ ) <sub>max</sub>	0.000, 0.001	0.000, 0.001	0.000, 0.001	0.000, 0.000
min. and max. residual density, e Å <sup>-3</sup>	-0.48, 0.54 [near Ru]	-0.46, 0.74 [near Ru]	-1.07, 0.90 [near Ru]	-1.06, 0.63 [near Ru]

<sup>a</sup>  $R = \sum ||F_o| - |F_c|| / \sum |F_o|$ . <sup>b</sup>  $wR2 = [\sum [w(F_o^2 - F_c^2)^2] / \sum [w(F_o^2)^2]]^{1/2}$ . <sup>c</sup>  $P = (\text{Max}(F_o^2, 0) + 2F_c^2) / 3$ .

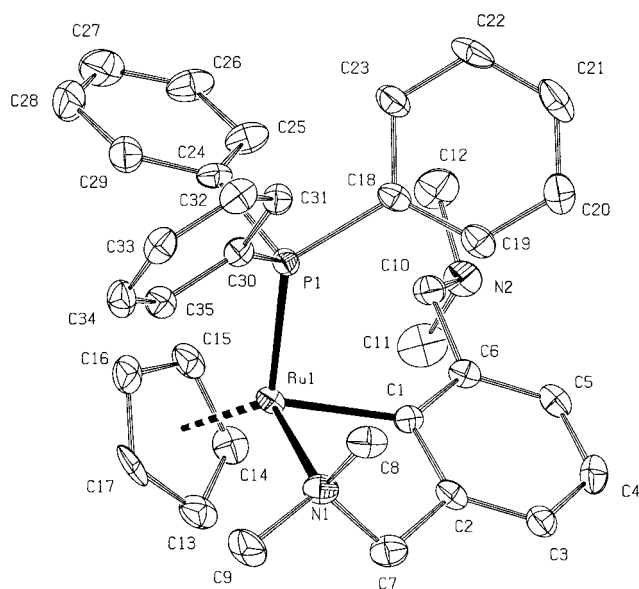


**Figure 4.** ORTEP drawing (50% probability atomic displacement ellipsoids) of the solid-state structure of [Ru(η<sup>5</sup>-Cp){η<sup>2</sup>-C,N-C<sub>6</sub>H<sub>3</sub>(CH<sub>2</sub>NMe<sub>2</sub>)<sub>2</sub>-2,6}(PPh<sub>3</sub>)] **5**. Hydrogen atoms have been omitted for clarity.

(1)}{LSQ} = 3.1(3)° for **5**. The five-membered chelate ring appears to be strained in both **5** and **6**; the sp<sup>2</sup> carbon atom C(1) in **5** and C(3) in **6** affords a Ru-C-C

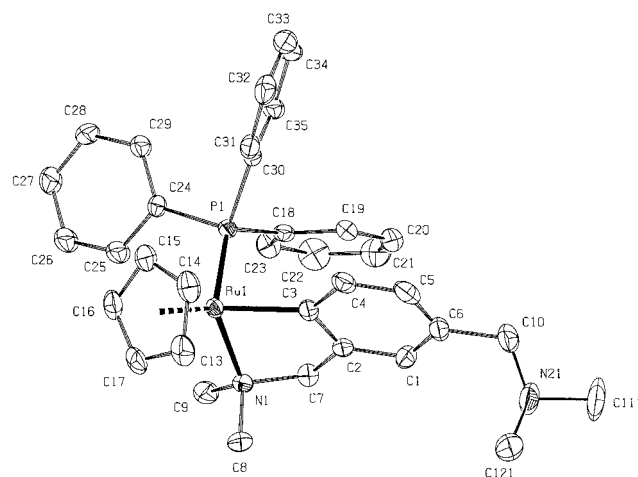


**Figure 5.** ORTEP drawing (50% probability atomic displacement ellipsoids) of the solid-state structure of [Ru(η<sup>5</sup>-Cp){η<sup>2</sup>-C,N-C<sub>6</sub>H<sub>3</sub>(CH<sub>2</sub>NMe<sub>2</sub>)<sub>2</sub>-2,4}(PPh<sub>3</sub>)] **6**. Hydrogen atoms and the minor disorder component of the free -CH<sub>2</sub>-NMe<sub>2</sub> group have been omitted for clarity.

angle of 114.5(4)° for **5**, again similar to **6**. As a consequence, the atom positioned *para* to the C<sub>ipso</sub>-Ru bond provides a C...C-Ru angle of 170.9(3)° (**5**) and 172.6(7)° (**6**). The molecular geometry of **5** also provides evidence for steric interference between the PPh<sub>3</sub> ligand and the noncoordinated CH<sub>2</sub>NMe<sub>2</sub> group. For example,

the phenyl carbon atom C(30) and the NMe proton H(8) are only separated by 2.59(3) Å, and this is 0.31 Å shorter than the sum of the van der Waals radii.

Comparison of these structural parameters indicates that in **6** there is less strain than that indicated for **5**. This view is corroborated by the P(1)–Ru(1)–C(3) bond angle of 89.13(13)° in **6**, which is close to the expected 90° of an undistorted octahedral ligand array and less than the corresponding angle of 97.28(15)° in **5**. Another indication that **6** is energetically more favorable than **5** comes from the fact that **6**, unlike **5**, does not show interference of the PPh<sub>3</sub> ligand with the noncoordinated –CH<sub>2</sub>NMe<sub>2</sub> group.

## Discussion

The present study has shown that the monoanionic NCN ligand [C<sub>6</sub>H<sub>3</sub>(CH<sub>2</sub>NMe<sub>2</sub>)<sub>2-2,6</sub>]<sup>–</sup> in **2** and **5** can rearrange in a highly selective manner to the [C<sub>6</sub>H<sub>3</sub>(CH<sub>2</sub>NMe<sub>2</sub>)<sub>2-2,4</sub>]<sup>–</sup> form in a process that involves the formation and cleavage of both aromatic and aliphatic C–H bonds.<sup>14–16</sup> On the basis of these results, it is possible to construct a likely mechanistic pathway that is consistent with rearrangements found in related ligand rearrangement reactions.<sup>1b,8a,b</sup> A relevant aspect when considering this type of rearrangement is the identification of a likely driving force. On the basis of the crystallographic and variable-temperature NMR results, the relief of steric strain is a likely cause for the conversion of **2** and **5**. For example, the solid-state structures of **3** and **6** establish specific coordination sphere bond angles that are significantly different from those of **2** and **5**, with the latter species clearly being more sterically congested. Specifically for **2**, this is reflected in close contacts of the *p*-cymene ligand with the noncoordinated –CH<sub>2</sub>NMe<sub>2</sub> group and in the unfavorable positioning of the Ru–Cl bond. In solution, the NMR spectroscopic data of **2** clearly show that there is a rotational barrier for the *p*-cymene ligand around the metal center–C<sub>6</sub> centroid axis. The corresponding data for complex **5** indicate steric strain in the C(1)–Ru(1)–P(1) interbond angle in addition to close contact between the noncoordinated NMe<sub>2</sub> function and a phenyl ring. In **3** and **6**, the amount of steric strain present appears to be greatly reduced. Recent work by Pfeffer and others has included detailed discussions of steric effects in substituted *ortho*-metalated organometallic complexes containing bidentate *C,N*-arylamines, e.g., [RuCl{C<sub>6</sub>H<sub>4</sub>(CH{Me}NMe<sub>2</sub>)<sub>2-2-C,N</sub>}(η<sup>6</sup>-C<sub>6</sub>H<sub>14</sub>)].<sup>9a–c,e,15a</sup> One can envision that **2**, **3**, **5**, and **6** can be viewed as derivatives of the well-known dmba ligand: [C<sub>6</sub>H<sub>4</sub>(CH<sub>2</sub>NMe<sub>2</sub>)<sub>2-2</sub>]<sup>–</sup>. In complexes **2** and **5**, the sterically bulky

–CH<sub>2</sub>NMe<sub>2</sub> group is positioned *ortho* to the metal center, whereas in the ligand-rearranged isomers **3** and **6** this group is positioned *para* to the metal center, causing less steric congestion.

Earlier studies employing NCN and related ligands with iridium(I)<sup>1a,8a</sup> and tantalum(V)<sup>1b,8b</sup> centers have also established overall rearrangement reactions of the ligand systems that are similar to those described here. A common feature of all the complexes that show this type of behavior is that they contain an η<sup>2</sup>-*C,N*-bonded ligand system in which there is a nonbonded sterically bulky substituent, e.g., CH<sub>2</sub>NMe<sub>2</sub>, positioned *ortho* to the metal to carbon σ-bond. Such a group has a steric bulk similar to that of an isobutyl fragment, and the η<sup>2</sup>-*C,N* bonding mode of the ligand holds this *ortho*-substituent in a fixed position relative to the metal center. In this location, the CH<sub>2</sub>NMe<sub>2</sub> substituent can obviously interfere with other ligands in the metal coordination sphere.

**Mechanistic Considerations.** The kinetic data of the rearrangement of **5** to **6** would appear to indicate an intramolecular mechanism. The absence of a kinetic isotope effect in the rearrangement of **5** (–*d*<sub>3</sub>) to **6** (–*d*<sub>3</sub>) indicates that the rate-determining step does not involve a C–H(D) bond formation or a cleavage reaction. Finally, any proposed mechanism has to account for the different H/D scrambling behavior found in the rearrangements of **2-d**<sub>3</sub> and **5-d**<sub>3</sub>.

On the basis of the above, a seven-step mechanism is proposed for the rearrangement of both complexes **2** and **5** to **3** and **6**, respectively. This is shown in Scheme 5. The first step in this mechanism is Ru–N bond dissociation to afford intermediate **A**. The change from η<sup>2</sup>-*C,N* to η<sup>1</sup>-*C* bonding of the aryldiamine ligand has been shown to occur at the onset of structural rearrangement in complexes of iridium(I)<sup>1a,8a</sup> and in complexes of the general formula [M{C<sub>6</sub>H<sub>3</sub>(CH<sub>2</sub>NMe<sub>2</sub>)<sub>2-2-C,N</sub>-R-6}(COD)] (M = Rh, Ir; R = H, Me, CH<sub>2</sub>NMe<sub>2</sub>; COD = cycloocta-1,5-diene). These compounds exhibit fluxional behavior induced by rupture of a M–N bond.<sup>8a,14</sup> In the mechanistic proposal herein, Ru–N bond dissociation is followed by methyl C–H bond activation of a NMe<sub>2</sub> group<sup>16</sup> that affords intermediate **B**. This occurs via oxidative addition and thus implies the intermediate formation of a NCH<sub>2</sub>–Ru<sup>IV</sup>–H unit. Subsequently, there is Ru–C bond cleavage on the aromatic ring via reductive elimination of the C<sub>aryl</sub>–Ru<sup>IV</sup>–H fragment and subsequent formation of a C<sub>aryl</sub>–H bond. This process forms intermediate **C**. In the next step, the metal-containing unit shifts from the original 1-position of the NCN ligand, along the π-system of the aryl nucleus, to the 3-position to afford intermediate **D**. This is followed by an aromatic C–H bond activation, via oxidative addition, to afford intermediate **E**, which contains another NCH<sub>2</sub>–Ru<sup>IV</sup>–H fragment (cf. **B**). Prior to the last step, there is reductive elimination from this unit with formation of a nonbonded NMe<sub>2</sub> group, i.e., **F**. In this intermediate, recoordination of an *ortho*-CH<sub>2</sub>NMe<sub>2</sub> substituent affords complexes **3** or **6**.

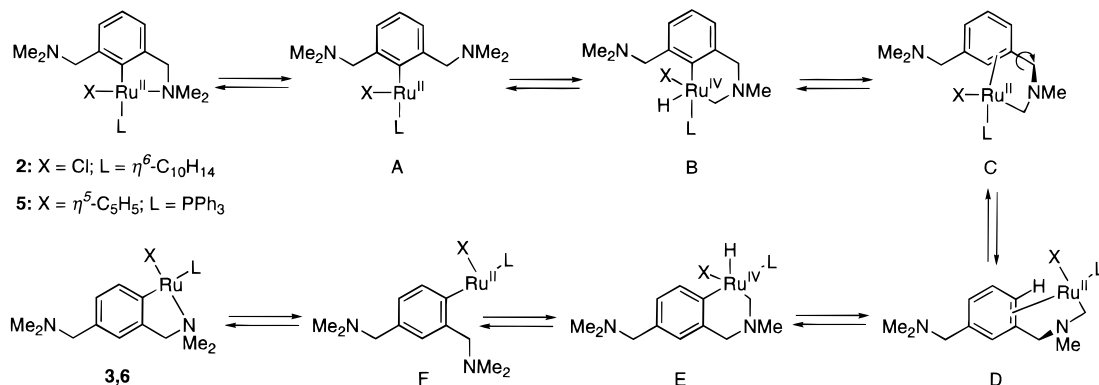
The fact that the onset temperatures for the rearrangement reactions of **2** and **5** are very close to each other indicates that these complexes have similar activation energies. This is consistent with the rupture

(14) van der Zeijden, A. A. H.; van Koten, G.; Nordemann, R. A.; Kojic-Prodic, B.; Spek, A. L. *Organometallics* **1988**, *7*, 1957.

(15) (a) Pfeffer, M. *Pure Appl. Chem.* **1992**, *64*, 335. Also see: (b) Steenwinkel, P.; Gossage, R. A.; van Koten, G. *Chem. Eur. J.* **1998**, *4*, 764, and references therein.

(16) (a) Mauthner, K.; Slugovc, C.; Mereiter, K.; Schmid, R.; Kirchner, K. *Organometallics* **1997**, *16*, 1956. (b) Slugovc, C.; Wiede, P.; Mereiter, K.; Schmid, R.; Kirchner, K. *Ibid.* **1997**, *16*, 2768. (c) Bertuleit, A.; Fritze, C.; Erker, G.; Fröhlich, R. *Ibid.* **1997**, *16*, 2891. (d) Abbenhuis, H. C. L.; Grove, D. M.; van Mier, G. P. M.; Spek, A. L.; van Koten, G. *Recl. Trav. Chim. Pays-Bas* **1990**, *109*, 361. (e) Abbenhuis, H. C. L.; van Belzen, R.; Grove, D. M.; Klomp, A. J. A.; van Mier, G. P. M.; Spek, A. L.; van Koten, G. *Organometallics* **1993**, *12*, 210. (f) Castro, I.; Galakhov, M. V.; Gómez, M.; Gómez-Sal, P.; Royo, P. *Ibid.* **1996**, *15*, 1362. (g) Gemel, C.; Mereiter, K.; Schmid, R.; Kirchner, K. *Ibid.* **1997**, *16*, 5601.

**Scheme 5. Proposed Mechanism for the Thermal Rearrangement Reaction of Complexes 2 and 5 to Complexes 3 and 6, Respectively. Note that for the Conversion of 2 to 3 the Formation of B from A Is Not Reversible (See Text)**

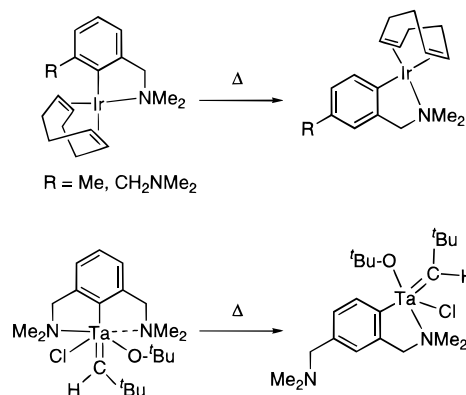


of energetically similar Ru–N bonds. The initial conversion of the NCN ligand from  $\eta^2\text{-C,N}$  to an  $\eta^1\text{-C}$ -bonding generates an electron-deficient metal center, and this is the important factor for the subsequent oxidative addition of a methyl group. Recall that the rearrangement reactions of **2** to **3** and **5** to **6**, respectively, are both solvent dependent, and this corroborates with Ru–N bond cleavage, where solvation energies play an important role.

Using the mechanism shown in Scheme 5, one can readily explain the different H/D scrambling behavior found for the rearrangement of **2-d<sub>3</sub>** to **3-d<sub>3</sub>** and for **5-d<sub>3</sub>** to **6-d<sub>3</sub>** in terms of reversible and irreversible steps. In the isomerization of **2** (-d<sub>3</sub>) to **3** (-d<sub>3</sub>), the noncoordinated  $\text{-CH}_2\text{NMe}_2$  group shows no deuterium incorporation, and this indicates that the conversion of **2** to **A** is irreversible (Scheme 5). If this were not so, it would be possible for both of the noncoordinated  $\text{-CH}_2\text{NMe}_2$  groups in **A** to become involved in C–H bond activation, whereby deuterium incorporation would occur in all four methyl groups. A direct consequence of this would also be hydrogen incorporation on the aromatic ring at both C atoms *ortho* to the noncoordinated  $\text{-CH}_2\text{NMe}_2$  group in **3-d<sub>3</sub>**. This is not the case. However, the second scenario is exactly what one encounters in the conversion of **5-d<sub>3</sub>** to **6-d<sub>3</sub>**; that is, both the coordinated and the noncoordinated  $\text{-CH}_2\text{NMe}_2$  groups of **6-d<sub>3</sub>** showed deuterium incorporation. This gives strong evidence that steps from **A** to **6** are reversible. The differences in (ir)reversibility of the steps in the rearrangement of **2** and **5** are obviously related to the electronic and steric differences in the ligand pairs:  $[\text{Cl}^-]/p\text{-cymene}$  on one hand and  $\text{PPh}_3/[\text{C}_5\text{H}_5]^-$  on the other. For the latter pair, the oxidative addition (**A** to **B**) and the reductive elimination (**E** to **F**) have to be reversible. This could mean that the transition states between **A** and **B** and between **E** and **F** are more stabilized (i.e., lower in energy) with the  $\text{PPh}_3/[\text{C}_5\text{H}_5]^-$  pair than with the  $[\text{Cl}^-]/p\text{-cymene}$  pair. This difference probably lies in the fact that the former pair has overall stronger donor and weaker accepting properties than the latter one.

This mechanistic proposal is similar to that described previously for the NCN complex  $[\text{M}\{\text{C}_6\text{H}_3(\text{CH}_2\text{NMe}_2)\text{-2-C,N-R-6}\}(\text{COD})]$  mentioned above, i.e., M–N bond rupture and a sequence of aromatic and aliphatic C–H bond activation processes.<sup>1a,8a</sup> In this latter study it was shown that after M–N bond rupture, the resulting

**Scheme 6. Reported Ligand Rearrangement Reactions of NCN Complexes of Iridium(I) and Tantalum(V)<sup>1a,8</sup>**



T-shaped intermediate could undergo either (i) rotation of the aryl fragment about the M–C<sub>aryl</sub> axis followed by recoordination of one of the N-donor groups (M = Rh; R =  $\text{CH}_2\text{NMe}_2$ ) or (ii) irreversible rearrangement of the starting material to the 2,4-isomer  $[\text{M}\{\text{C}_6\text{H}_3(\text{CH}_2\text{NMe}_2)\text{-2-C,N-R-4}\}(\text{COD})]$  (M = Ir; see Scheme 6). In this study, there is no spectroscopic evidence for an aryl rotation step that would lead to equivalence of the bonded and nonbonded  $\text{CH}_2\text{NMe}_2$  groups in **2**. However, this cannot be exclusively ruled out in the case of **5**, specifically in the conversion of **5** to intermediate **A** (vide supra).

A related 2,6- to 2,4-rearrangement of the NCN ligand has also been identified in Ta(V) chemistry involving the complex  $[\text{Ta}(\text{=CH-}^t\text{Bu})\{\text{C}_6\text{H}_3(\text{CH}_2\text{NMe}_2)\text{-2,6-C,N}\}(\text{O-}^t\text{Bu})_2]$ , but this rearrangement (Scheme 6) has been shown to follow an entirely different mechanism from that discussed above.<sup>1b,8b</sup> A  $\sigma$ -bond metathesis reaction of the alkylidene fragment and the C<sub>aryl</sub>–Ta bond affords an intermediate tantalum alkylidyne species and a new C<sub>aryl</sub>–H unit. The latter bond is formed through protonation of C<sub>ipso</sub> that is mediated by the noncoordinated  $\text{-CH}_2\text{NMe}_2$  substituent acting as an intramolecular Lewis base. In the final step, a second  $\sigma$ -bond metathesis reaction leads to the product containing the rearranged NCN ligand.

The high thermal stability of complex **9**, when compared to that of complex **2**, can be attributed to the absence of a C–H bond at aromatic C-3 of the  $\text{C}_2\text{N}_4$  ligand. Furthermore, dissociation of a Ru–N bond,



which would be a likely initial step in fluxionality or complex reactivity, is hindered by steric buttressing<sup>17</sup> of the adjacent *ortho*-positioned CH<sub>2</sub>NMe<sub>2</sub> substituents. This implies that any rearrangement process would require intermediates such as **B–D** (see Scheme 5). This is obviously not possible for **9**.

Complexes **2** and **5**, as well as the Ta(V) and Ir(I) complexes described above, isomerize through processes that involve the transition metal induced activation of aliphatic and/or aromatic C–H bonds. Crabtree and Hamilton,<sup>18</sup> Jones and Feher,<sup>19</sup> and Ryabov and Van Eldik<sup>20</sup> have comprehensively reviewed this area of organometallic chemistry. The activation of C–H bonds described by these authors is believed to proceed via a prior agostic interaction of the C–H bond with a metal center before bond activation occurs.<sup>21</sup> Intramolecular C–H bond activation (i.e., cyclometalation) involving platinum group metal compounds has been reviewed,<sup>15</sup> and extensive studies of ruthenium(II),<sup>9a,22</sup> rhodium(III),<sup>23</sup> and palladium(II)<sup>9d,24</sup> have been performed. This work has strongly suggested that such direct cyclometalation reactions are electrophilic in nature<sup>9</sup> and that after the agostic interaction of the C–H bond, the next step involves formation of an arenium-type intermediate.<sup>25</sup> The relevance of this form of an intermediate in the rearrangement reactions of **2** to **3** and **5** to **6** is that such a species could well be a transition state between the intermediates **B** and **C** and between **D** and **E** (Scheme 5). In related platinum(II) chemistry, it has been demonstrated that arenium species are not only feasible but also isolable.<sup>1a,2c</sup> This class of electrophilic metalation postulated in this mechanistic scheme can also be used for direct synthetic purposes starting from compounds such as the precursor to NCN: [1,3-bis-(dimethylaminomethyl)benzene]. When this compound is reacted with [RuCl<sub>2</sub>( $\eta^6$ -C<sub>10</sub>H<sub>14</sub>)]<sub>2</sub> (Scheme 1), a direct cyclometalation occurs selectively at the 4-position to provide complex **3**, i.e., an isomer of **2**. Thus, we have shown that one of the crucial steps in the mechanism of the rearrangement reaction of complexes **2** and **5** can be used synthetically to directly prepare organoruthenium(II) complexes of the “rearranged” NCN ligand (i.e., the thermodynamically more stable isomer).

## Conclusions

It has been shown that the monoanionic NCN ligand can be successfully used in the synthesis of new organometallic Ru(II) complexes through two different synthetic strategies. One of these approaches, involving lithiation and transmetalation, can also be used in the synthesis of a 1,4-phenylene-bridged bisruthenium(II) complex derived from the related dianionic C<sub>2</sub>N<sub>4</sub> ligand. The NCN complexes described here are sterically congested species that are thermally stable under mild conditions in nonpolar solvents. However, these compounds rearrange to the less congested complexes upon heating or when dissolved in polar solvents. The operational rearrangement process is apparently a selective intramolecular one that involves aliphatic and aromatic C–H bond activation. These reactions have provided a new approach to the synthesis of organoruthenium complexes of *C,N*- and *N,C,N*-chelating ligands via procedures that involve direct cyclometalation.

In addition, the knowledge of the rearrangement mechanism provides information that should allow for better control of substrate and product selectivity when aryldiamine ligands are used in both stoichiometric<sup>9b,c</sup> and catalytic<sup>1b</sup> metal-mediated synthesis. Reaction conditions that cause an NCN ligand rearrangement should clearly be avoided since this is likely to adversely affect catalytic performance. This study indicates that nonbulky spectator ligands such as CO may be preferable to those present in **2** and **5**. In fact, the higher thermal stability of complex **9**, in which the metal centers are bidentate *C,N*-coordinated (cf. **2** and **5**), most likely as a result of steric buttressing of the CH<sub>2</sub>NMe<sub>2</sub> ligands, is an important observation that may provide a new starting point for the design of improved homogeneous catalysts. Further research in this area is currently in progress.

## Experimental Section

All organometallic syntheses were performed in a dry nitrogen atmosphere, using standard Schlenk techniques. The solvents were dried and freshly distilled prior to use. The <sup>1</sup>H, <sup>2</sup>H, <sup>13</sup>C{<sup>1</sup>H}, and <sup>31</sup>P{<sup>1</sup>H} NMR experiments were performed at 298 K with Bruker AC200 or AC300 spectrometers, unless otherwise stated. Chemical shifts ( $\delta$ ) are given in ppm, relative to SiMe<sub>4</sub> or external 85% aqueous H<sub>3</sub>PO<sub>4</sub>. Elemental analyses were carried out by Dornis und Kölbe, Mikroanalytisches Laboratorium, Mülheim, Germany. The compounds [Li{C<sub>6</sub>H<sub>3</sub>(CH<sub>2</sub>NMe<sub>2</sub>)<sub>2</sub>-2,6}]<sub>2</sub>, <sup>1,26</sup> [RuCl{C<sub>6</sub>H<sub>3</sub>(CH<sub>2</sub>NMe<sub>2</sub>)<sub>2</sub>-2,6-*N,C,N'*}(PPh<sub>3</sub>)], **4**,<sup>3a</sup> [RuCl<sub>2</sub>( $\eta^6$ -C<sub>10</sub>H<sub>14</sub>)]<sub>2</sub>,<sup>27</sup> and [RuCl<sub>2</sub>(PPh<sub>3</sub>)<sub>4</sub>]<sup>28</sup> were prepared according to literature procedures.

### Synthesis of [RuCl{C<sub>6</sub>H<sub>3</sub>(CH<sub>2</sub>NMe<sub>2</sub>)<sub>2</sub>-2,6-*C,N'*}( $\eta^6$ -C<sub>10</sub>H<sub>14</sub>)]

**(2).** A solution of **1** (0.93 g, 2.35 mmol) in Et<sub>2</sub>O (25 mL) was added dropwise over a period of 5 min to a stirred suspension of [RuCl<sub>2</sub>( $\eta^6$ -C<sub>10</sub>H<sub>14</sub>)]<sub>2</sub> (1.44 g, 2.35 mmol) in Et<sub>2</sub>O (50 mL) at

(17) (a) Menger, F. M. *Acc. Chem. Res.* **1985**, *18*, 128. (b) Brown, J. M.; Pearson, M.; Jastrzebski, J. T. B. H.; van Koten, G. *J. Chem. Soc., Chem. Commun.* **1992**, 1440.

(18) Crabtree, R. H.; Hamilton, D. G. *Adv. Organomet. Chem.* **1988**, *28*, 299.

(19) Jones, W. D.; Feher, F. J. *Acc. Chem. Res.* **1989**, *22*, 91.

(20) (a) Ryabov, A. D. *Chem. Rev.* **1990**, *90*, 403. (b) Ryabov, A. D.; van Eldik, R. *Angew. Chem., Int. Ed. Engl.* **1994**, *33*, 783.

(21) Brookhart, M.; Green, M. L. H. *J. Organomet. Chem.* **1983**, *250*, 395.

(22) For C–H bond activation reactions of C<sub>6</sub>H<sub>3</sub>(CH<sub>2</sub>PPh<sub>2</sub>)<sub>2</sub>-1,3-R-5 (R = H, Ph) with ruthenium(II) complexes see: (a) Karlen, T.; Dani, P.; Grove, D. M.; Steenwinkel, P.; van Koten, G. *Organometallics* **1996**, *15*, 5687. (b) Dani, P.; Karlen, T.; Gossage, R. A.; Smeets, W. J. J.; Spek, A. L.; van Koten, G. *J. Am. Chem. Soc.* **1997**, *119*, 11317. (c) Jia, G.; Lee, H. M.; Xia, H. B.; Williams, I. D. *Organometallics* **1996**, *15*, 5453.

(23) For rhodium(III)-mediated C–H bond activation reactions of C<sub>6</sub>H<sub>4</sub>(CH<sub>2</sub>NMe<sub>2</sub>)<sub>2</sub>-1,3 see: (a) van der Zeijden, A. A. H.; van Koten, G.; Luijk, R.; Vrieze, K.; Slob, C.; Krabbendam, H.; Spek, A. L. *Inorg. Chem.* **1988**, *27*, 1014. (b) Hiraki, K.; Fuchita, Y.; Ohta, Y.; Tsutsumida, J.; Hardcastle, K. I. *J. Chem. Soc., Dalton Trans.* **1992**, 833.

(24) For C–H bond activation reactions of (dimethylamino)methyl-substituted arenes with palladium(II) salts see: (a) Valk, J.-M.; Maassarani, F.; van der Sluis, P.; Spek, A. L.; Boersma, J.; van Koten, G. *Organometallics* **1994**, *13*, 2320. (b) Valk, J.-M.; van Belzen, R.; Boersma, J.; Spek, A. L.; van Koten, G. *J. Chem. Soc., Dalton Trans.* **1994**, 2293. (c) Alsters, P. L.; Engel, P. F.; Hogerheide, M. P.; Copijn, M.; Spek, A. L.; van Koten, G. *Organometallics* **1993**, *12*, 1831.

(25) Canty, A. J.; van Koten, G. *Acc. Chem. Res.* **1995**, *28*, 406.

(26) (a) Grove, D. M.; van Koten, G.; Louwen, J. N.; Noltes, J. G.; Spek, A. L.; Ubbels, H. J. C. *J. Am. Chem. Soc.* **1982**, *104*, 6609. (b) Jastrzebski, J. T. B. H.; van Koten, G.; Konijn, M.; Stam, C. H. *Ibid.* **1982**, *104*, 5490.

(27) Bennett, M. A.; Smith, A. K. *J. Chem. Soc., Dalton Trans.* **1974**, 233.

(28) Hallman, P. S.; Stephenson, T. A.; Wilkinson, G. *Inorg. Synth.* **1970**, *12*, 237.

0 °C. The reaction mixture was allowed to warm to RT and then stirred for 24 h at this temperature. The reaction mixture was then evaporated in vacuo to dryness. The brown-yellow solid residue was washed with pentane (2 × 50 mL) and extracted with benzene (4 × 50 mL). The combined benzene extracts were evaporated in vacuo yielding a red-brown powder, identified as **2**, which was deemed to be of sufficient purity for further use (yield: 1.83 g; 84%). Analytically pure orange crystals of **2** (mp 128–129 °C, dec), which were suitable for X-ray analysis, were obtained by slow diffusion of pentane into a concentrated solution of **2** in THF. Anal. Calcd for [C<sub>22</sub>H<sub>33</sub>ClN<sub>2</sub>Ru] (MW = 462.07): C, 57.19; H, 7.20; N, 6.06. Found: C, 57.14; H, 7.12; N, 6.15.

**Synthesis of [Ru( $\eta^5$ -Cp){C<sub>6</sub>H<sub>3</sub>(CH<sub>2</sub>NMe<sub>2</sub>)<sub>2</sub>-2,6-C,N}-(PPh<sub>3</sub>)] (**5**).** A solution of freshly prepared [Na(Cp)]<sub>n</sub> (0.29 g, 3.29 mmol) in THF (4 mL) was added dropwise over a period of 2 min to a dark blue solution of **4**<sup>3a</sup> (1.34 g, 2.27 mmol) in THF (25 mL) at –78 °C. The reaction mixture was then allowed to warm to RT over a period of 1 h and stirred for 14 h, during which time the color of the reaction mixture changed from blue to yellow. The yellow suspension that had formed was quenched with CH<sub>2</sub>Cl<sub>2</sub> (5 mL), and all volatiles were evaporated in vacuo to leave behind a dark yellow residue. The crude product was extracted with benzene (2 × 50 mL). The combined benzene extracts were concentrated to ca. 10 mL and layered with pentane, yielding **5** as a yellow solid (yield: 1.05 g; 75%). Analytically pure orange crystals were obtained by cooling a pentane/benzene (19:1, v/v) solution to –25 °C, mp 141–143 °C (dec). Anal. Calcd for [C<sub>35</sub>H<sub>39</sub>N<sub>2</sub>PRu + 2/3 C<sub>6</sub>H<sub>6</sub>] (MW = 671.86): C, 69.72; H, 6.45; N, 4.17. Found: C, 69.89; H, 6.47; N, 3.95.

**Rearrangement of **2** to [RuCl{C<sub>6</sub>H<sub>3</sub>(CH<sub>2</sub>NMe<sub>2</sub>)<sub>2</sub>-2,4-C,N}( $\eta^6$ -C<sub>10</sub>H<sub>14</sub>)] (**3**).** A yellow solution of **2** (100 mg, 0.22 mmol) in C<sub>6</sub>H<sub>6</sub> (50 mL) was heated at reflux for 3 h, while the color changed from yellow to orange-yellow. Following this procedure, all volatiles were removed in vacuo, leaving a brown powder. This residue was washed with Et<sub>2</sub>O (2 × 25 mL) and then dried in vacuo. Yield: 74 mg (74%) of **3** as a red-brown powder. Analytically pure orange crystals of **3** (mp 132–136 °C, dec), which were suitable for an X-ray analysis, were obtained by slow evaporation (in air) of a solution of **3** in a mixture of CH<sub>2</sub>Cl<sub>2</sub> and MeOH (1:5 v/v). Anal. Calcd for [C<sub>22</sub>H<sub>33</sub>ClN<sub>2</sub>Ru + 1/4 CH<sub>2</sub>Cl<sub>2</sub>] (MW = 483.31): C, 55.30; H, 6.99; N, 5.80. Found: C, 55.45; H, 6.98; N, 5.56.

**Independent Synthesis of **3**.** Solid NaPF<sub>6</sub> (0.30 g, 1.4 mmol) was added to a solution of 1,3-bis[(dimethylamino)methyl]benzene (0.27 g, 1.4 mmol) and [RuCl<sub>2</sub>( $\eta^6$ -C<sub>10</sub>H<sub>14</sub>)<sub>2</sub>] (0.43 g, 0.7 mmol) in CH<sub>2</sub>Cl<sub>2</sub> (10 mL), and this mixture was stirred at RT for 18 h. After filtration, the solution was separated by column chromatography using silica and CH<sub>2</sub>Cl<sub>2</sub> as eluent. A yellow band, which eluted slowly, was collected and concentrated to ca. 5 mL. Then MeOH (2 mL) was added, and the solution was slowly evaporated in air. Analytically pure orange crystals of **3** were collected from the dark brown solution by filtration and were then dried in vacuo. Yield: 0.17 g (27%).

**Rearrangement of **5** to [Ru( $\eta^5$ -Cp){C<sub>6</sub>H<sub>3</sub>(CH<sub>2</sub>NMe<sub>2</sub>)<sub>2</sub>-2,4-C,N}(PPh<sub>3</sub>)] (**6**).** A yellow solution of **5** (0.18 g, 0.29 mmol) in C<sub>6</sub>H<sub>6</sub> (100 mL) was heated at reflux temperature for 2.5 h; no color change was observed. The solvent was removed in vacuo, leaving a yellow solid, identified as **6**. Analytically pure orange crystals of **6** (mp 150–152 °C, dec), which were suitable for an X-ray analysis, were obtained by cooling a pentane/benzene (19:1, v/v) solution to –25 °C. Anal. Calcd for [C<sub>35</sub>H<sub>39</sub>N<sub>2</sub>PRu + 1/3 C<sub>6</sub>H<sub>6</sub>] (MW = 645.82): C, 68.81; H, 6.40; N, 4.34. Found: C, 68.88; H, 6.40; N, 4.02.

**Synthesis of [1,4-{RuCl( $\eta^6$ -C<sub>10</sub>H<sub>14</sub>)<sub>2</sub>}{C<sub>6</sub>(CH<sub>2</sub>NMe<sub>2</sub>)<sub>4</sub>-2,3,5,6-C,N-C,N}]] (**9**).** A solution of *n*-BuLi (1.5 mL, 1.6 M in hexanes, 2.4 mmol) was added dropwise over a period of 2 min to a suspension of **7** (0.51 g, 1.1 mmol) in Et<sub>2</sub>O (20 mL) at –78 °C. The reaction mixture was stirred for 15 min at –78

°C, then allowed to warm to RT over a period of 30 min, and then stirred at this temperature for an additional 30 min. The white precipitate that had formed, the arylidilithium reagent **8**, was collected by centrifugation, washed with Et<sub>2</sub>O (50 mL), and suspended in THF (20 mL). To this suspension was added a suspension of [RuCl<sub>2</sub>( $\eta^6$ -C<sub>10</sub>H<sub>14</sub>)<sub>2</sub>] (0.61 g, 2 mmol of Ru) in THF (20 mL) at RT through a knee-tube. This mixture was stirred at RT until all the solids had dissolved (1 h) and then left undisturbed for 18 h, after which a dark red-brown solid had precipitated. The solid was filtered off, washed with Et<sub>2</sub>O (20 mL), and extracted with CH<sub>2</sub>Cl<sub>2</sub> (2 × 50 mL). Evaporation of the combined CH<sub>2</sub>Cl<sub>2</sub> extracts to dryness afforded **9** as an orange-brown solid, which was recrystallized from CH<sub>2</sub>Cl<sub>2</sub> by slow addition of Et<sub>2</sub>O. Yield: 0.32 g (38%) of orange-brown crystals, mp 146–149 °C (dec). A reproducible combustion analysis could not be obtained for this material.

**Synthesis of C<sub>6</sub>D<sub>3</sub>Br-Me<sub>2</sub>-2,6.** A modification of a described procedure was used.<sup>29</sup> A vigorously stirred mixture of bromo-2,6-xylene (14.9 g, 80.5 mmol), D<sub>2</sub>O (3 mL, 167 mmol), and D<sub>2</sub>SO<sub>4</sub> (11 mL, 200 mmol) was heated at reflux for three 1 min intervals and subsequently stirred for 15 h at RT. The gray suspension that had formed was diluted with a saturated aqueous solution of NaCl (25 mL), and this mixture was extracted with CH<sub>2</sub>Cl<sub>2</sub> (4 × 50 mL). The combined CH<sub>2</sub>Cl<sub>2</sub> extracts were dried with MgSO<sub>4</sub> and filtered, and the filtrate was concentrated in vacuo to leave a colorless oil. This procedure was repeated five times, until a deuterium enrichment of the aryl group of ca. 99% (as determined by <sup>1</sup>H NMR integration) was obtained. After purification by flash distillation the product was obtained as a colorless oil (10.8 g, 71%). <sup>1</sup>H NMR (200 MHz, CDCl<sub>3</sub>):  $\delta$  = 2.45 (s, CH<sub>3</sub>).

**Synthesis of C<sub>6</sub>D<sub>3</sub>Br(CH<sub>2</sub>Br)<sub>2</sub>-2,6.**<sup>10</sup> A mixture of C<sub>6</sub>D<sub>3</sub>-Br-Me<sub>2</sub>-2,6 (10.8 g, 57.7 mmol), NBS (22.6 g, 127 mmol), and AIBN (1.0 g, 6 mmol) in methyl acetate (200 mL) was heated at reflux temperature under illumination (100 W bulb) for 15 h. The solvent was then removed in vacuo, and the orange oily residue was extracted with boiling hexane (4 × 100 mL). The product crystallized from the combined hexane extracts on cooling to –25 °C. Yield: 10.8 g (55%) of a white solid (mp 85–88 °C, dec). <sup>1</sup>H NMR (200 MHz, CDCl<sub>3</sub>):  $\delta$  = 4.65 (s, CH<sub>2</sub>-Br).<sup>3b</sup>

**Synthesis of C<sub>6</sub>D<sub>3</sub>Br(CH<sub>2</sub>NMe<sub>2</sub>)<sub>2</sub>-2,6.** Neat HNMe<sub>2</sub> (18 mL, 0.27 mol) was added to a stirred solution of C<sub>6</sub>D<sub>3</sub>Br(CH<sub>2</sub>-Br)<sub>2</sub>-2,6 (10.8 g, 32 mmol) in Et<sub>2</sub>O (200 mL) at 0 °C. The reaction mixture was stirred at this temperature for 2 h. The mixture was then allowed to warm to RT and stirred for an additional 14 h. All volatiles were evaporated in vacuo, and then an aqueous solution of NaOH (100 mL, 2.5 M) was added to the remaining white, solid residue. The mixture was extracted with hexane (2 × 100 mL), the combined hexane fractions were dried with MgSO<sub>4</sub> and filtered, and the filtrate was concentrated in vacuo. After flash distillation of the pale yellow oily residue the product was obtained as a colorless oil, which slowly solidified upon standing at –25 °C. Yield: 7.4 g (84%). <sup>1</sup>H NMR (200 MHz, CDCl<sub>3</sub>):  $\delta$  = 3.50 (s, 4 H, CH<sub>2</sub>N), 2.26 (s, 12 H, NCH<sub>3</sub>). <sup>2</sup>H NMR (31 MHz, C<sub>6</sub>H<sub>6</sub>):  $\delta$  = 7.3 (s, 2 D, ArD), 6.9 (s, 1 D, ArD). <sup>13</sup>C{<sup>1</sup>H} NMR (50 MHz, CDCl<sub>3</sub>):  $\delta$  = 138.6 (s, C<sub>ortho</sub>), 129.0 (t, <sup>1</sup>J<sub>DC</sub> = 25 Hz, C<sub>meta</sub>), 126.7 (s, CBr), 126.1 (t, <sup>1</sup>J<sub>DC</sub> = 25 Hz, C<sub>para</sub>), 63.9 (s, CH<sub>2</sub>N), 45.6 (s, NCH<sub>3</sub>).

**Synthesis of [RuCl{C<sub>6</sub>D<sub>3</sub>(CH<sub>2</sub>NMe<sub>2</sub>)<sub>2</sub>-2,6-C,N}( $\eta^6$ -C<sub>10</sub>H<sub>14</sub>)] (**2-d<sub>5</sub>**).** This complex was prepared using the method described for the preparation of complex **2**, but now starting from [Li{C<sub>6</sub>D<sub>3</sub>(CH<sub>2</sub>NMe<sub>2</sub>)<sub>2</sub>-2,6}]<sub>2</sub>, **1-d<sub>3</sub>**, which was prepared in situ in Et<sub>2</sub>O from C<sub>6</sub>D<sub>3</sub>Br(CH<sub>2</sub>NMe<sub>2</sub>)<sub>2</sub>-2,6 and 2 equiv of *t*-BuLi at –78 °C.

**Synthesis of [RuCl{C<sub>6</sub>D<sub>3</sub>(CH<sub>2</sub>NMe<sub>2</sub>)<sub>2</sub>-2,6-N,C,N}(PPh<sub>3</sub>)] (**4-d<sub>5</sub>**).** This complex was prepared using the method described for the synthesis of **4**,<sup>3a</sup> but now starting from [Li{C<sub>6</sub>D<sub>3</sub>(CH<sub>2</sub>-

(29) van der Zeijden, A. A. H.; van Koten, G.; Luijk, R.; Nordemann, R. A.; Spek, A. L. *Organometallics* **1988**, 7, 1549.

$\text{NMe}_2)_2\text{-2,6}\}_2$ , which was prepared in situ in THF from  $\text{C}_6\text{D}_3\text{-Br}(\text{CH}_2\text{NMe}_2)_2\text{-2,6}$  and 2 equiv of *t*-BuLi at  $-78^\circ\text{C}$ .

**Synthesis of  $[\text{Ru}(\eta^5\text{-Cp})\{\text{C}_6\text{D}_3(\text{CH}_2\text{NMe}_2)_2\text{-2,6-C,N}\}(\text{PPh}_3)]$  (**5-d<sub>3</sub>**).** This complex was prepared using the method described for the synthesis of complex **5**, but now starting from the deuterated complex **4-d<sub>3</sub>**.

**Rearrangement of **2-d<sub>3</sub>** to  $[\text{RuCl}\{\text{C}_6\text{D}_2\text{H}(\text{CH}_2\text{NMe}_2\text{-D})_2\text{-2,4-C,N}\}(\eta^6\text{-C}_{10}\text{H}_{14})]$  (**3-d<sub>3</sub>**).** The method was identical to that described for the rearrangement reaction of complex **2** to **3**, starting from **2-d<sub>3</sub>**.

**Rearrangement of **5-d<sub>3</sub>** to  $[\text{Ru}(\eta^5\text{-Cp})\{\text{C}_6\text{H}_2\text{D}(\text{CH}_2\text{N}(\text{CH}_2\text{D})\text{Me})_2\text{-2,4-C,N}\}(\text{PPh}_3)]$  (**6-d<sub>3</sub>**).** The method was identical to that described for the rearrangement reaction of complex **5** to **6**.

**Kinetic Experiments.** The conversion of complex **5** to **6** as a solution in  $\text{C}_6\text{H}_6$  at concentrations of 0.70 and 6.75 mmol/L was monitored by  $^1\text{H}$  NMR spectroscopy. The conversion of complex **2** to **3** as a solution in  $\text{C}_6\text{H}_6$  at concentrations of 10 and 48 mmol/L was also monitored by  $^1\text{H}$  NMR spectroscopy. The conversion rates were obtained by following the decrease of the intensities of the *p*-cymene resonances (**2**) and of the  $\text{C}_5\text{H}_5$  singlet resonances (**5**). At 3 min time intervals samples of the solutions were evaporated in vacuo, dissolved in  $\text{C}_6\text{D}_6$ , and analyzed by  $^1\text{H}$  NMR spectroscopy. An internal standard was employed.

**X-ray Structure Determination of Complexes **2**, **3**, **5**, and **6**.** Crystals suitable for X-ray diffraction were mounted on the tip of a glass fiber and were placed in the cold nitrogen stream on an Enraf-Nonius CAD4-T diffractometer on a rotating anode (Mo  $\text{K}\alpha$  radiation, graphite monochromator,  $\lambda = 0.71073$ ). Accurate unit cell parameters and an orientation matrix were determined by least-squares fitting of the setting angles of a set of well-centered reflections (SET4<sup>30</sup>). The unit cell parameters were checked for the presence of higher lattice symmetry.<sup>31</sup> Crystal data and details of data collection and refinement are collected in Table 3. All data were collected at 150 K in  $\omega$  scan mode. Data were corrected for *Lp* effects and for the observed linear decay of the reference reflections, but not for absorption.

The structure of **5** was solved by automated direct methods (SHELXS-86<sup>32</sup>); the structures of the other complexes were solved by automated Patterson methods and subsequent difference Fourier techniques (DIRDIF-92<sup>33</sup>). The structures were refined on  $F^2$ , using full-matrix least-squares techniques

(SHELXL-96<sup>34</sup> for complex **6** and SHELXL-93<sup>35</sup> for the other complexes); no observance criterion was applied during refinement.

Hydrogen atoms were included in the refinement on calculated positions, riding on their carrier atoms. For complexes **5** and **6** the C–H bond length was included as a refinement parameter. All methyl hydrogen atoms were refined in a rigid group allowing for rotation around the C–C and C–N bonds. The  $\text{CH}_2\text{N}(21)\text{Me}_2$  group of complex **6** was found to be disordered over two positions. The site occupancy parameter of the major disorder component refined to 0.820(7). Weak distance constraints were applied to enforce the same bond distances and angles for both disorder components.

The non-hydrogen atoms were refined with anisotropic thermal parameters, except for the disordered atoms of **6**. The thermal parameter of the minor disorder component atoms were equivalenced to the equivalent isotropic displacement parameters of the corresponding major disorder component atoms. The hydrogen atoms were refined with a fixed isotropic thermal parameter related to the value of the equivalent isotropic displacement parameter of their carrier atoms.

Neutral atom scattering factors and anomalous dispersion corrections were taken from the International Tables for Crystallography.<sup>36</sup> Geometrical calculations and illustrations were performed with PLATON;<sup>37</sup> all calculations were performed on a DECstation 5000 cluster.

**Acknowledgment.** This work was supported in part (P.S., H.K., W.J.J.S., and A.L.S.) by The Netherlands Foundation for Chemical Research (SON) with financial aid from The Netherlands Organization for Scientific Research (NWO). We would like to thank Mr. Arun M. Rambocus and Mr. Göran Verspui for their contributions to part of this investigation.

**Supporting Information Available:** Tables of all positional parameters, thermal parameters, and bond lengths and bond angles for **2**, **3**, **5**, and **6** (29 pages). Ordering information is given on any current masthead page including instructions on how to access this information via the Internet.

OM980343U

(30) de Boer, J. L.; Duisenberg, A. J. M. *Acta Crystallogr.* **1984**, *A40*, C410.

(31) Spek, A. L. *J. Appl. Crystallogr.* **1988**, *21*, 578.

(32) Sheldrick, G. M. *SHELXS-86 Program for crystal structure determination*; University of Göttingen, Germany, 1986.

(33) Beurskens, P. T.; Admiraal, G.; Beurskens, G.; Bosman, W. P.; García-Granda, S.; Gould, R. O.; Smits, J. M. M.; Smykalla, C. *The DIRDIF program system, Technical report of the Crystallography Laboratory*; University of Nijmegen, The Netherlands, 1992.

(34) Sheldrick, G. M. *SHELXL-96 Program for crystal structure refinement*; University of Göttingen, Germany, 1996.

(35) Sheldrick, G. M. *SHELXL-93 Program for crystal structure refinement*; University of Göttingen, Germany, 1993.

(36) Wilson, A. J. C., Ed. *International Tables for Crystallography*, Vol. C; Kluwer: Dordrecht, The Netherlands, 1992.

(37) Spek, A. L. *Acta Crystallogr.* **1990**, *A46*, C34.